Mass Transfer, Energy-Exergy Analysis, and Mathematical Modeling of Chili Pepper During Drying

Agarry, Samuel Enahoro*[+]

Biochemical and Bioenvironmental Laboratory, Department of Chemical Engineering, Ladoke Akintola University of Technology, Ogbomoso, NIGERIA

Osuolale, Funmilayo Nihinola

Process System Engineering Laboratory, Department of Chemical Engineering, Ladoke Akintola University of Technology, Ogbomoso, NIGERIA

Agbede, Oluseye Omoseye

Separation Processes/Unit Operation Laboratory, Department of Chemical Engineering, Ladoke Akintola University of Technology, Ogbomoso, NIGERIA

Ajani, Ayobami

Biochemical and Bioenvironmental Laboratory, Department of Chemical Engineering, Ladoke Akintola University of Technology, Ogbomoso, NIGERIA

Afolabi, Tinuade Jolaade

Separation Processes/Unit Operation Laboratory, Department of Chemical Engineering, Ladoke Akintola University of Technology, Ogbomoso, NIGERIA

Ogunleye, Oladipupo Olaosebikan

Process System Engineering Laboratory, Department of Chemical Engineering, Ladoke Akintola University of Technology, Ogbomoso, NIGERIA

Ajuebor, Felix

Federal Institute of Industrial Research, Oshodi, Lagos, NIGERIA

ABSTRACT: *There are no literature data on the effects of air velocity and relative humidity on moisture diffusivity, mass transfer coefficient, and energy-exergy analysis of chili pepper during cabinet-tray hot-air drying. This study tends to address this gap by presenting comprehensive drying kinetic, energy, and exergy analyses of a cabinet-tray hot-air drying for red chili pepper. Drying was conducted at varying levels of air temperature (40-70 ^{o}C), air velocity (0.5-2.0 m/s), and relative humidity (60-75%). The effect of drying conditions on drying time, drying coefficient, lag factor, drying efficiency, moisture ratio, effective moisture diffusivity, mass transfer coefficient, Total Energy Consumption (TEC), Specific Energy Consumption (SEC), Energy Utilization Ratio (EUR), heat loss,*

***** *To whom correspondence should be addressed.*
+ *E-mail: seagarry@lautech.edu.ng*
1021-9986/2022/7/2468-2495 20/$/2.00

energy efficiency, exergy loss, exergy efficiency, Exergetic Improvement Potential (EIP), and Exergy Sustainability Index (ESI)) was evaluated. Five different mass transfer models (Dincer-Dost, Bi-Di, Bi-S, Bi-G, and Bi-Re) were applied to determine the mass transfer parameters. A new drying mathematical model was developed for the prediction of drying kinetic, energy, and exergy parameters. Effective moisture diffusivity values of 1.58×10^{-8} - 5.10×10^{-8} m^2/s and mass transfer coefficient values of 0.053×10^{-6} - 8.79×10^{-6} m/s over the drying conditions range were respectively obtained. The TEC, SEC, and EUR achieved over the range of drying conditions in the course of drying were in the range of 43.56-77.36 MJ, 49.0-87.02 MJ/kg, and 0.035-0.325, respectively. Heat loss and exergy loss varied from 0.16 to 2.39 MJ and from 0.026 to 0.622 kW, respectively. Drying, energy, and exergetic efficiency values obtained varied in the range of 2.80-8.25%, 2.69-7.91%, and 73-94.5%, respectively. EIP and the ESI values varied from 0.0068-0.114 kW and 3.70-18.18, respectively. The developed multivariate linear regression model provided an innovative model to predict drying kinetic, energy, and exergy parameters.

KEYWORDS: *Chili pepper; Drying conditions; Energy and exergy parameters; Mass transfer models; Moisture transfer parameters; Multivariate linear regression model.*

INTRODUCTION

Chili pepper is a highly nutritive fruit that contains several macronutrients and micronutrients [1] that can be used as spices and flavor in a dried and ground form [2]. However, the fruit is seasonal with high moisture content, highly perishable with a short shelf life of 2 to 3 days, and high post-harvest loss or wastage [3, 4]. One of the methods adopted for reducing these losses and extending the shelf life is to reduce the moisture content/water activity through the method of drying. Several researchers have investigated the drying of chili pepper using different methods of drying based on the type of drying equipment such as solar drying [5], convective tray drying [6], infra-red drying [7], vacuum drying [8], rotary drying [9], and fluidized bed drying [10]. Although fluidized beds, infra-red, microwave, rotary, and vacuum drying produce a very good quality product in terms of nutritional composition, color, texture, and flavor, however, they suffer from the problem of high cost [11]. Nevertheless, majorly for easy drying operation, a faster rate of drying, affordability, and bulk or large-scale economical drying of chili pepper, convective air drying happens to be the most appropriate drying method [11].

Drying is a complex, unsteady, nonlinear, and dynamic process in which the kinetics are dependent on factors such as the type of material and its properties, dimensions, and shapes of the material, the type of drying method (based on drying equipment type), and the drying process conditions [12, 13]. Drying kinetics is therefore a complex phenomenon that requires simple mathematical models or representations necessary for predicting and optimizing drying behavior and drying parameters as well as for dryer design, control, and energy integration [14, 15]. Since drying as a phenomenon simultaneously involves heat and mass transfer, obtaining an accurate spatial and temporal drying profile depends on the accuracy of the effective moisture diffusivity. Effective moisture diffusivity is the principal key variable that is used to describe moisture diffusion during the drying of agricultural food products [11]. This is because moisture diffusion is the food products' intrinsic moisture transport property, which includes capillary and hydrodynamic flow, surface diffusion, molecular diffusion, liquid, and vapor diffusion [15]. Fick's diffusion model has been the most widely used mass transfer model to describe mass transfer or moisture diffusion in food products [16]. However, other models and mathematical correlations such as Biot-Dincer (Bi-Di), Biot-Reynolds (Bi-Re), Biot-lag number (Bi-G), and Biot-drying coefficient (Bi-S) correlations have been proposed by some workers to describe moisture transfer in food products [17, 18]. Fick's diffusion equation takes into account only the internal moisture diffusion mechanism while the Bi-Di, Bi-Re, Bi-G, and Bi-S correlations take into account both external and internal diffusion mechanisms. Therefore, experimental and modeling investigations are still very necessary and important in the simulation, design, and control of the drying process.

Also, the drying operation is an energy-intensive operation and due to the high cost of energy and global warming, improving the efficiency of drying for good quality dried products involves the key issue of reducing energy consumption thereby reducing the cost of energy [19]. Thus the knowledge of the energy consumption of various drying systems is essential [19]. This knowledge is required for a more in-depth understanding of the drying process because more complex correlations and mathematical models depend on these data [15]. Many works have been done on moisture diffusivity, mass transfer coefficients, and energy consumption in the drying of several agricultural food products, such as apple [20], kiwi [21], plantain [22], rice [14], soybean [15], whole lemons [23], yam [24], Russian olive [25], and mint and parsley leaves [26].

Furthermore, thermodynamic analyses, and more particularly exergy analysis, have become an essential and necessary tool for the design of systems and evaluation as well as for thermal systems optimization [27]. From the focal viewpoint of thermodynamics, exergy being a parameter of the thermodynamics' second law is not subject to the law of conservation, thus it can be destroyed or consumed within the system due to irreversibility [28, 29]. Exergy helps to estimate the quantity of available energy at different points or locations as well as helps to determine the magnitudes and types of energy losses in a system [30]. A lot of studies have been done on the exergetic analyses of food products drying under different drying equipment such as convective tray drying of red pepper [31], coroba slices [32], olive leaves [27], onion [28, 33], microwave drying of soybean [15], fluidized bed drying of carrot [34], and solar-hot air drying of chili pepper [35].

Much research works have been carried out on varying aspects of the drying of different varieties of pepper such as green and red pepper [19, 31, 36, 37], red and green bell pepper [38, 39], and red and green chili pepper [35, 40, 41]. In all of these works, the major interest was to investigate drying methods, drying temperature, and pretreatment effects on physicochemical quality and drying kinetics. However, among the works, it was only *Akpinar* [31] that had investigated and evaluated the effect of temperature on the exergy and energy efficiencies of convective tray drying of red pepper, while *Rabha et al.* [35] studied and analyzed the exergy and energy of the solar-hot air drying of ghost chili pepper. Thus, literature reports on energy consumption (i.e. energy analysis), moisture diffusivity, and exergy analysis of chili pepper hot air drying with respect to the use of the convective cabinet-tray drying method are still very limited.

With regards to drying conditions, only a few researchers have investigated the effects of both drying air velocity and temperature on the energy and exergy consumption or utilization of agricultural and food products drying using drying equipment such as mixed flow dryers [42], solar hybrid dryers [43], and convective tray dryers [27, 28], while very few workers have evaluated the effect of relative humidity on energy consumption [24, 44] and exergetic efficiency [45]. However, to the best of our knowledge, there are no information and literature data on the effects of air velocity and relative humidity on moisture transport parameters (moisture diffusivity and mass transfer coefficient) and energy-exergy consumption of convective cabinet-tray drying of chili pepper. The range of relative humidity values that has mostly been studied as a drying condition in the drying of food products as observed from the literature lies between 10 and 60% [24, 46 – 48]. In this study, the authors would investigate the effect of higher values of relative humidity that range from 60 to 75% at a fixed high drying air temperature of 70 ^{o}C and air velocity of 2 m/s which have seldom been studied.

Therefore, due to these research gaps observed from the detailed literature review conducted in this present study, the objectives of this current research work were to: (1) determine the drying kinetic parameters (drying time, drying coefficient, and lag factor); (2) determine the parameters of mass transfer (moisture diffusivity and mass transfer coefficient) using five different comparative mass transfer models; (3) provide energy-exergy (thermodynamic) analyses of convective cabinet-tray drying of chili pepper to determine Total Energy Consumption (TEC), Specific Energy Consumption (SEC), Energy Utilization Ratio (EUR), heat loss, energy efficiency, exergy loss, exergy efficiency, Exergetic Improvement Potential (EIP), and Exergy Sustainability Index (ESI); (4) develop a mathematical model for the prediction and estimation of drying process parameters (drying time, drying coefficient, and lag factor), moisture content profile, energy, and exergy parameters; and (5) evaluate the effects of drying process conditions (drying air temperature, drying air velocity, and relative humidity)

on the drying kinetic parameters (drying time, drying coefficient, lag factor), mass transfer parameters (moisture diffusivity and moisture transfer coefficient), energy parameters (TEC, SEC, heat loss, and energy efficiency), and exergy parameters (exergy loss, exergy efficiency, EIP, and, ESI). The results from this study will serve as a baseline to provide useful information that will facilitate the design and development of an efficient large-scale drying system for the chili pepper industry with improved throughput and reduced energy consumption.

EXPERIMENTAL SECTION

Preparation of material

Fresh Nigerian red chili pepper (Fig. 1) utilized for this research was purchased from a local market at Lagos (6.5219° N, 3.3565° E), Nigeria. The samples were sorted out, and those of similar size, shape, and color were selected and kept in a refrigerator (Haier Thermocool, HR 134BS, Nigeria) at 4 ºC before drying. The native chili pepper samples were brought out from the refrigerator and allowed to equilibrate with the surrounding ambient temperature for 2 hours before usage [20].

Chili pepper drying

The drying of the chili pepper was carried out using a self-designed cabinet-tray dryer fabricated at Ladoke Akintola University of Technology, Ogbomoso, Nigeria, and having a control volume of 0.34 m^3 (Fig. 2).

The description of the dryer has been presented elsewhere [49]. The drying of the chili pepper was carried out using the one variable-at-a-time (OVAT) procedure where one variable is varied and the other variables are kept constant. The drying process was carried out at a drying air temperature range (40, 50, 60, and 70 ºC), drying air velocity (0.5, 1.0, 1.5, and 2.0 m/s), and relative humidity (60, 65, 70, and 75%), respectively. In this procedure, the fresh red chili pepper samples were sliced into a 2 mm thickness and 1 kg of the samples were weighed with a digital precision balance (Sartorius Secura1103-1Sar, Germany with ±0.001 mg accuracy) and spread on the clean tray of the cabinet dryer. The dryer was heated to the required drying temperature before the tray was placed into the dryer chamber. The drying was carried out according to the experimental design in Table 1.

Fig. 1: A sample of Nigerian fresh chili pepper.

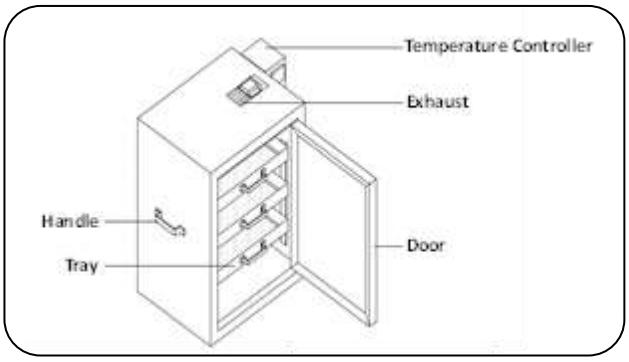

Fig. 2: A cabinet-tray dryer for the drying of plantain slices.

Humidification of the drying air entering the drying chamber was performed using a water aerosol (i.e. 1L water trigger sprayer (Sprayon Model SO-075)) manually operated behind the air blower until the desired relative air humidity was attained. The ambient temperature, outlet temperatures of the drying chamber walls, and the product as well as the relative humidity were measured and recorded with a dual-function instrument (PCE-555 Model, Southampton, United Kingdom with ±0.1 ºC temperature accuracy and ±2% relative humidity accuracy) that measures both temperature and relative humidity, respectively. The velocity of the air delivered by the air-blower was measured using a hot-wire anemometer (PCE-009 Model, Southampton, United Kingdom). At intervals of 30 min, the mass loss of the samples was measured by making use of a digital precision analytical balance until a constant weight was achieved. This procedure does not last for more than 20 s [50]. The moisture content was measured according to the standard method [51]. In triplicates, each of the experiments performed and the average moisture content values were utilized for the plotting of the drying kinetics curves. The initial moisture content of the Nigerian red chili pepper was obtained to be 84.98% (wet basis) or 5.66 kg water/kg dry

Table 1: OVAT design of experiment utilized for the convective cabinet hot air drying of red chili pepper.

Experimental Run	Drying Air Temperature (°C)	Drying Air Velocity (m/s)	Relative Humidity (%)
1	40	2	60
2	50	2	60
3	60	2	60
4	70	2	60
5	70	0.5	60
6	70	1.0	60
7	70	1.5	60
8	70	2.0	60
9	70	2.0	60
10	70	2.0	65
11	70	2.0	70
12	70	2.0	75

matter (dry basis). The final moisture content of the dried red chili pepper after the drying process was found to be 9.02% (wet basis) or 0.099 kg water/kg dry matter (dry basis) while the equilibrium moisture content was obtained to be relatively very small (0.006 kg water/kg dry matter) since it took a long time to attain the final moisture content of 9.02%.

Mathematical modeling of mass transfer

Mass transfer model I (Dincer and Dost model)

The moisture diffusion process that occurs during the drying of a moist solid material is similar to the heat conduction that occurs in such a moist material. Hence, the governing second law of diffusion equation given by Fick that defines moisture diffusion for a moist solid material is in the same form as the heat transfer Fourier equation, in which temperature and thermal diffusivity are respectively replaced with moisture and moisture diffusivity. Therefore, in determining the effective moisture diffusivity, the chili pepper was considered as an infinite slab or rectangular and the following assumptions were made: (1) the thermo-physical properties of the drying air medium and sample are constant, (2) the effect of the transfer of heat on the mass or moisture transfer is negligible, (3) there are both internal and external resistances to the moisture diffusion within the sample (i.e. 0 < Bi < 100), and (4) moisture diffusivity occurs in a unidirectional form along the thickness of the slab. With the above-stated conditions, one-dimensional rectangular coordinates of the time-dependent moisture diffusivity equation can be written as follows:

$$\frac{\partial M}{\partial z} = \frac{1}{D_{eff}} \frac{\partial M}{\partial t} \tag{1}$$

Where $M = M_t - M_{eq}$ having an initial and boundary conditions of:

$M(z,0) = M_o$ = Constant

$$\left(\frac{\partial}{\partial z} M(0, t) \right) = 0 \quad \text{at } z = 0$$

$$-D_{eff} \left(\frac{\partial}{\partial z} M(L, t) \right) = K \left(M(L,t) - M_o \right) \quad \text{at } z = L$$

The solution to the moisture transfer governing Eq. (1) is given as follows [52]:

$$MR = \sum_{n=1}^{\infty} A_n B_n \quad For\ 0 < Bi < 100\ and\ Bi > 100 \tag{2}$$

MR, is the normalized moisture content or dimensionless moisture ratio and is expressed as given in Eq. (3):

$$MR = \frac{M_t - M_{eq}}{M_o - M_{eq}} \tag{3}$$

Eq. (2) can be simplified when the values of the Fourier number are very small and thus negligible (i.e. Fo > 0.2). That means the period of constant rate is neglected and therefore the first term in Eq. (2) is used to approximate the infinite sum and expressed as follows [52]:

$$MR = A_1 B_1 \tag{4}$$

Where

$$A_1 = \exp\left(\frac{0.2533Bi}{1.3 + Bi} \right) \tag{5}$$

$$B_1 = \exp\left(-\mu_1^2 Fo \right) \tag{6}$$

μ_1 depends on the sample geometry and is calculated using Eq. (7) for a slab geometry [17, 24]:

$$\mu_1 = -419.24G^4 + 2103.8G^3 - 3615.8G^2 + 2880.3G - 858.94 \tag{7}$$

$$Fo = \frac{D_{eff}\, t}{L^2} \quad (8)$$

The dimensionless moisture ratio in Eq. (4) can be written in the exponential form in terms of drying coefficient (*S*) and lag factor (*G*) as given in Eq. (9) [24, 52]:

$$MR = G\exp(-St) \quad (9)$$

The drying coefficient (*S*) and lag factor (*G*) can be obtained from the non-linear regression of moisture ratio and time using the least-square curve fitting method [24]. The goodness of fit was determined using the correlation coefficient (R^2). The drying coefficient relates to the drying capacity of a moist solid material per unit of time while the lag factor is an indicator in the moist solid material that relates to the internal resistance to moisture transport during drying [24]. Equations (4) and (9) are in the same form and can therefore be equated to each other with ($G = A_1$) and exp(-St) = B_1. Therefore Eq. (4) becomes:

$$MR = \exp\left(0.2533Bi/1.3 + Bi\right) * \exp(-St) \quad (10)$$

Mass transfer model II (Bi - Di correlation)

The moisture distribution or transfer can be modeled using the Biot number-Dincer number (*Bi-Di*) correlation given in Eq. (11) [24]:

$$Bi = 24.848Di^{-0.375} \quad (11a)$$

Biot number (*Bi*) is a dimensionless parameter in drying that indicates the resistance to moisture transfer or diffusion within the moist solid material. It is a function of both moist solid material and drying air medium properties. The Dincer number (*Di*) which is a dimensionless number, depicts the impact of the air flow velocity (V) of the drying medium on the drying coefficient of the moist solid material during drying. This was mathematically expressed as follows [24]:

$$Di = \frac{V}{SL} \quad (11b)$$

Mass transfer model III (Bi - Re correlation)

The moisture distribution or transfer can also be modeled using the Biot number-Reynolds number (Bi-Re) correlation given in Eq. (12) [17]:

$$Bi = 22.55Re^{-0.59} \quad (12a)$$

$$Re = \frac{\rho_{da} V L}{\nu} \quad (12b)$$

The viscosity (ν) can be estimated using Eq. (13) [53]:

$$\nu = 1.718\times10^{-5} + 4.62\times10^{-8}T \quad (13)$$

Mass transfer model IV (Bi-S correlation)

The Biot number–drying coefficient (*Bi-S*) correlation is expressed as follows [17]:

$$Bi = 1.2388S^{0.333} \quad (14)$$

Mass transfer model V ($Bi - G$ correlation)

The Biot number and Lag factor correlation ($Bi\text{-}G_{correlation}$) is as given in Eq. (15) [18]:

$$Bi = 0.0576G^{26.7} \quad (15)$$

Determination of effective moisture diffusivity and mass transfer coefficient

The effective moisture diffusivity (D_{eff}) in m^2/s can be deduced using Eq. (16) [17, 24]:

$$D_{eff} = \frac{Sy^2}{\mu_1^2} \quad (16)$$

With the use of moisture transfer models II to V, μ_1 for a slab geometry can be calculated using Eq. (17) [17, 24]:

$$\mu_1 = -419.24G^4 + 2103.8G^3 - 3615.8G^2 + 2880.3G - 858.94 \quad (17)$$

The mass transfer coefficient (K_m) in m/s can be obtained using Eq. (18):

$$K_m = \frac{BiD_{eff}}{y} \quad (18)$$

The first law of thermodynamics: Total and specific energy consumption

By the application of the first law of thermodynamics (which states that energy entering a thermal system is conserved and cannot be destroyed), the drying process was analyzed based on the steady flow conservation of mass (for dry air and moisture in the dry air) and the conservation of energy utilizing the following equations:

The general equation for energy balance [27]:

$$\sum E_{in} = \sum E_{out} \quad (19a)$$

$$\sum E_{in} = \dot{m}_{dai} h_{dai} + \dot{m}_{FP} h_{FP} \quad (19b)$$

$$\sum E_{out} = \dot{m}_{dao} h_{dao} + \dot{m}_{DP} h_{DP} + \dot{Q}_{Loss} \quad (19c)$$

According to the conservation of mass, the total mass entering into the drying chamber is equal to the total mass leaving the drying chamber hence, it was assumed that $\dot{m}_{dai} = \dot{m}_{dao} = \dot{m}_{da}$ $\dot{m}_{FP} = \dot{m}_{DP} = \dot{m}_{P}$ [27], therefore the energy utilization (Q_U) during the red chili pepper drying can be calculated using Eq. (20) [43, 54]:

$$Q_U = \dot{m}_{da}(h_{dai} - h_{dao}) + \dot{m}_{P}(h_{FP} - h_{DP}) - \dot{Q}_{Loss} \quad (20)$$

Where h_{dai} and h_{dao} are the enthalpies of the inlet and outlet drying air, respectively; while h_{FP} and h_{DP} are the enthalpies of the fresh and dried chili pepper, respectively.

Enthalpy of the fresh and dried chili pepper can be expressed as [43]:

$$h_P = C_{mp}(T_P - T_\infty) \quad (21)$$

C_{mp}, is the specific heat of wet food material which can be estimated using Eq. (22) [55]:

$$C_{mp} = 0.83736 + 3.348M \quad (22)$$

Heat loss ($\dot{Q}_{Loss}$), which is the rate of heat transfer to the environment can be obtained from the utilization of Eq. (23a) [43, 54]:

$$\dot{Q}_{Loss} = U_D A_D (T_{Dav} - T_\infty) \quad (23a)$$

The heat loss coefficient (U_D) can be calculated using Eq. (23b) [43, 54]:

$$U_D = \frac{\dot{m}_{da} C_{pda}(T_i - T_o)}{A_D (T_{Dav} - T_\infty)} \quad (23b)$$

The specific heat capacity of drying air (C_{pda}) can be estimated with the use of Eq. (23c) [28, 43, 56]:

$$C_{pda} = 1.004 + 1.88w \quad (23c)$$

The Energy Utilization Ratio (EUR) can be calculated from the use of Eq. (24) [43]:

$$EUR = \frac{\dot{m}_{da}(h_{dai} - h_{dao}) + \dot{m}_{p}(h_{FP} - h_{DP}) - \dot{Q}_{Loss}}{\dot{m}_{da}(h_{dai} - h_{\infty})} \quad (24)$$

The energy transferred from the heater (E_H) to the drying air that enters the drying chamber can be estimated using Eq. (25) [57]:

$$E_H = \dot{m}_{da} C_{pda} \Delta T \quad (25)$$

The Total Energy Consumption (TEC) in the course of chili pepper drying can be estimated using Eq. (26) [57]:

$$TEC = \frac{(E_H + E_{AB}) \times t_T}{1000} \quad (26)$$

The Specific Energy Consumption (SEC) required to remove the unit mass (1 kg) of moisture from the chili pepper slices at each drying process condition was determined using Eq. (27) [55, 56]:

$$SEC = \frac{TEC}{m_w} \quad (27)$$

Energy and drying efficiencies

The energy efficiency (η_E) can be derived using Eq. (28) [20]:

$$\text{Energy Efficiency } (\eta_E) = \frac{Q_w}{TEC} \quad (28)$$

Q_w (Energy consumed for moisture evaporation (kJ)) is calculated using Eq. (29a) [20]:

$$Q_w = h_v \times m_w \quad (29a)$$

h_v (Latent heat of vaporization of free water) can be deduced using Eq. (29b) [15]:

$$h_v = 2503 - 2.386(T - 273) \quad (29b)$$

Drying efficiency can be determined using Eq. (30a) [20]:

$$\text{Drying Efficiency } (\eta_D) = \frac{Q_m + Q_w}{TEC} \quad (30a)$$

Q_m (Energy utilized for heating the sample, kJ) can be calculated using Eq. (30b):

$$Q_m = W_m C_{mp}(T_o - T_i) \quad (30b)$$

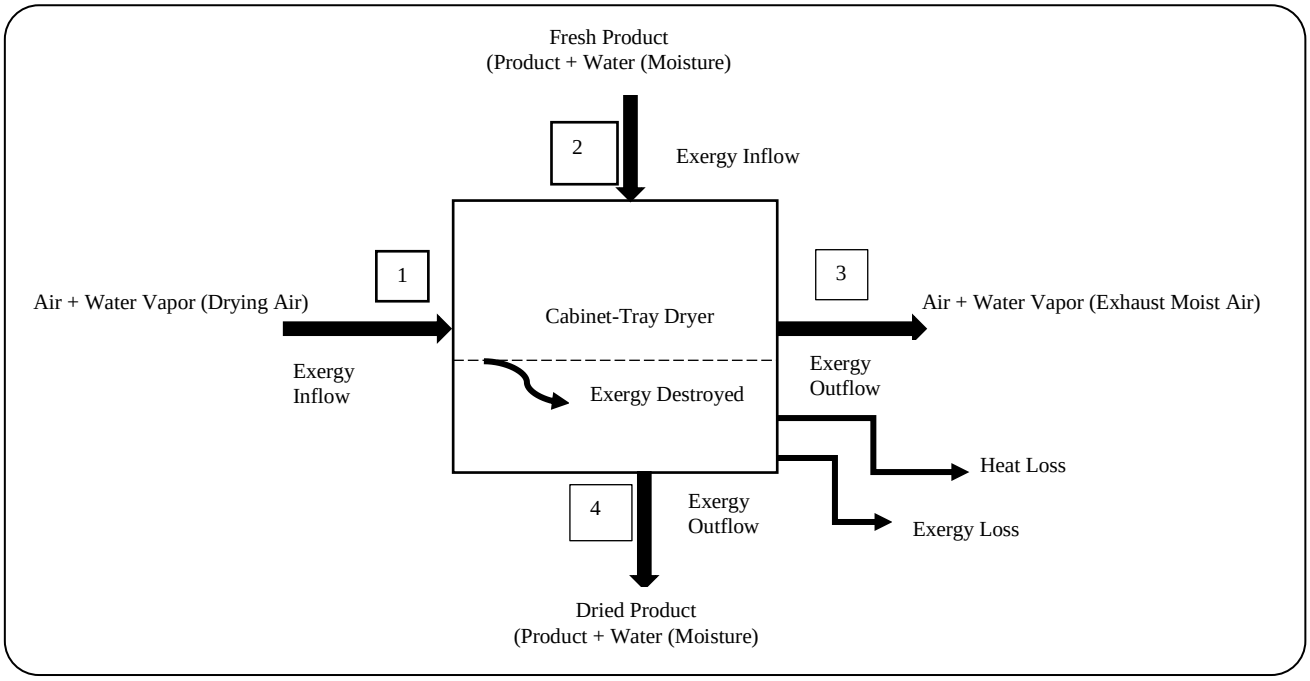

Fig. 3: Schematic diagram of the convective hot air drying process with inlet and outlet terms.

The second law of thermodynamics: Exergy analysis

Exergy is the energy that is available from any source [31]. The thermodynamics' second law was applied to carry out exergy analyses by estimating the total exergy inflow, outflow, and exergy losses of the convective cabinet-tray drying process that occurs in the drying chamber. Fig. 3 illustrates the schematic flow diagram of the convective cabinet-tray drying process that occurs in the drying chamber, indicating inlet and outlet terms.

To write the exergy balance equations for the cabinet-tray dryer illustrated in Fig. 3, three components such as the drying air, wet product, and moisture or water which exits with the drying air (exhaust moist air) and dried product were considered [27]. The general form of exergy balance is written as follows (29, 31):

Exergy = Internal energy + Entropy + Work + Momentum + Potential energy + Chemical energy + Radiation (31a)

$$\text{Exergy} = (u - u_\infty) - T_o(S - S_\infty) + P(v - v_\infty) + \quad (31b)$$

$$m\frac{V^2}{2} + mg(z - z_\infty) + \sum(\mu_{ch} - \mu_\infty)N_{ch}$$

$$\sigma A_i F_i\left(3T^4 - T_\infty^4 - 4T_\infty T^3\right) + \ldots\ldots\ldots$$

However, in writing the exergy equation for the above system (Fig. (3)), the following assumptions were made:

(1) The mass flow rate of drying air entering into the drying chamber is equal to the mass flow rate of exhaust air exiting from the drying chamber; (2) The effects of kinetic and potential (gravitational) energies of the system or flow of materials are negligible with no chemical and nuclear reactions of the material; and (3) The change in the pressure of drying air entering the drying chamber and the pressure of exhaust air leaving the drying chamber is negligible (i.e. $v \approx v_\infty$).

The internal energy and work can be replaced with enthalpy when considering a steady flow system [29, 31]. Therefore, the specific exergy for a steady flow system based on Eq. (31b) and on the above assumptions was expressed for the convective cabinet-tray drying process as follows [15, 30]:

$$ex = C_{pda}(T - T_\infty) - T_\infty\left\{C_{pda}\ln\left(\frac{T}{T_\infty}\right)\right\} \quad (32a)$$

The rate of exergy ($\dot{E}x$) (kJ/s or kW) was expressed as given in Eq. (32b) [27]:

$$\dot{E}x = \dot{m} \times ex \quad (32b)$$

Where $\dot{m}$ = mass flow rate (kg/s).

The exergy balance equation for the inflow and outflow terms can therefore be written as expressed in Eq. (33) [27]:

$$\sum \dot{E}x_{in} = \sum \dot{E}x_{out} + \sum \dot{E}x_{des} + \sum \dot{E}x_{Loss} - \sum \dot{E}x_{evap} \quad (33)$$

Therefore, the exergy inflow ($\dot{E}x_{in}$) and exergy outflow ($\dot{E}x_{out}$) rates as well as exergy flow rates due to destruction (or irreversibility) ($\dot{E}x_{des}$), evaporation ($\dot{E}x_{evap}$), and heat loss ($\dot{E}x_{Loss}$) based on Fig. 3 can be expressed as follows [27]:

$$\dot{E}x_{in} = \dot{m}_{da}\, ex_1 + \dot{m}_{mp}(ex_{mp})_2 + (\dot{m}_{wc})_2(ex_{wc})_2 \quad (34a)$$

$$\dot{E}x_{out} = \dot{m}_{da}\, ex_3 + \dot{m}_{mp}(ex_{mp})_4 + (\dot{m}_{wc})_4(ex_{wc})_4 \quad (34b)$$

$$\sum \dot{E}x_{des} = T_\infty S_{gen} \quad (34c)$$

$$\sum \dot{E}x_{evap} = \left(1 - \frac{T_\infty}{T_{mp}}\right)\dot{Q}_{evap} \quad (34d)$$

$$\sum \dot{E}x_{Loss} = \left(1 - \frac{T_\infty}{T_s}\right)\dot{Q}_{Loss} \quad (34e)$$

Employing Eq. (34a-b), and taking into account the moisture associated with the drying air (i.e. moist air), moist or wet product, and the water content, the exergy inflow and exergy outflow can be obtained depending on the inlet and outlet temperatures and levels of relative humidity (or humidity ratios) of the drying chamber. The specific exergy for the drying air (moist air), red chili pepper (fresh and dried), and moisture content can be obtained utilizing Eqs. (35a) - Eq. (35f), respectively.

$$ex_1 = ex_{dci} = \quad (35a)$$

$$\left(C_{pda} + w_1 C_{pwv}\right)(T_1 - T_\infty) - T_\infty\left(C_{pda} + w_1 C_{pwv}\right)\ln\left(\frac{T_1}{T_\infty}\right) +$$

$$T_\infty\left\{\left(R_{da} + w_1 R_{wv}\right)\ln\left(\frac{1 + 1.6078w^\infty}{1 + 1.6078w_1}\right) + 1.6978 w_1 R_{da}\ln\left(\frac{w_1}{w^\infty}\right)\right\}$$

The specific exergy associated with exhaust moist air or humid air exiting from the drying chamber is given as:

$$ex_3 = ex_{dco} = \quad (35b)$$

$$\left(C_{pda} + w_3 C_{pwv}\right)(T_3 - T_\infty) - T_\infty\left(C_{pda} + w_3 C_{pwv}\right)\ln\left(\frac{T_3}{T_\infty}\right) +$$

$$T_\infty\left\{\left(R_{da} + w_3 R_{wv}\right)\ln\left(\frac{1 + 1.6078w^\infty}{1 + 1.6078w_3}\right) + 1.6078 w_3 R_{da}\ln\left(\frac{w_3}{w^\infty}\right)\right\}$$

Specific exergy for the moist fresh and dried red chili pepper product is given as:

$$ex_{mp} = \left[(H - H^o) - T(S - S^o)\right] = \quad (35c)$$

$$[\hat{H}_p(T,P) - \hat{H}_p(T_\infty, P_\infty)] - T_\infty[S_p(T,P) - S_p(T_\infty, P_\infty)]$$

Where

$$(H - H^o) = \int_{T_\infty}^{T} C_{mp}\, dT = C_{mp}(T - T_\infty) \quad (35d)$$

and

$$(S - S^o) = \int_{T_\infty}^{T} \frac{C_{mp}}{T} dT = C_{mp}\ln\left(\frac{T}{T_\infty}\right) \quad (35e)$$

Specific exergy for moisture content is presented in Eq. (35f):

$$ex_{wc} = \left|[h_f(T) - h_g(T_\infty)] - [T_\infty(s_f(T) - s_g(T_\infty)]\right| + \quad (35f)$$

$$T_\infty R_{wv}\ln\left(\frac{T_\infty}{x^o_{wv}}\right)$$

The exergy efficiency (η_{Ex}) is defined as the ratio of the exergy losses (i.e. used exergy in the product drying) and the exergy inflow or input (i.e. drying air exergy supplied to the system) [43].

$$\eta_{Ex} = \frac{\sum \dot{E}x_{in} - \sum \dot{E}x_{Loss}}{\sum \dot{E}x_{in}} = \left(\frac{\sum \dot{E}x_{out}}{\sum \dot{E}x_{in}}\right) \times 100 \quad (36)$$

Different processes or economic sectors can be analyzed using the concept of Exergetic Improvement Potential (EIP). The exergetic improvement potential is obtained by using Eq. (37) [28]:

$$EIP = (1 - \eta_{Ex})\, Ex_{Loss} \quad (37)$$

The exergetic sustainability index (ESI) is an important exergy evaluation parameter [28]. This index allows for

Table 2: Measuring instruments and the uncertainties of measured parameters.

Instrument	Specifications	Accuracy	Parameter	Standard Deviation	Uncertainty (%)
Thermometer	PCE-555 Model, UK.	±0.5 ºC	Temperature	0.83	2.70
Anemometer	PCE-009 Model, UK.	±5%	Air Velocity	0.12	4.23
Hygrometer	PCE-555 Model, UK	±2%	Relative Humidity	1.99	3.56
Digital Balance	Sartorius Secura1103-1Sar, Germany	±0.001mg	Mass or Weight	0.07	0.06

information to be obtained about the influence or impact of the process on the environment. The ESI can be deduced from Eq. (38):

$$ESI = \frac{1}{1 - \eta_{Ex}} \tag{38}$$

The environmental impact factor decreases if the exergetic sustainability index increases [28]. The reference-dead state conditions were determined as $T_\infty = 30$ ºC, w= 0.015%, $C_{pwv} = 1.872$ kJ/kg.K, $R_{da} = 0.287$ kJ/kg.K, $R_{wv} = 0.4615$ kJ/kg.K, and $x^o_{wv} = 0.024$ were assumed as constant in all calculations. The thermodynamic properties of air and water were obtained from the steam tables.

Experimental uncertainty determination

Uncertainties in the experiments can come from the selection and condition of the measuring instrument, calibration, readings or measurement, observations, and environment [42]. Uncertainty analysis was performed to prove the accuracy and reproducibility of the data obtained during the chili pepper drying experiments. Drying air temperature, relative humidity, drying air velocity, and mass of the sample, were measured with the necessary and appropriate testing instruments, and the values were recorded. The mean or average of the recorded values obtained from the measurements and their standard deviations were determined. *Mondal et al*. [42] method was employed to determine the uncertainty of a value or variable X_i.

$$X_i = X_{mean} \pm \partial X_i \tag{39a}$$

The uncertainty percentage was calculated as follows:

$$\%\,Uncertainty = \frac{\partial X_i}{X_{mean}} \times 100 \tag{39b}$$

The estimated percent uncertainties for the instruments used in this study are provided in Table 1. An uncertainty value that is lower than 5% is considered to be acceptable for the reproducibility of an experiment [42]. It could be seen from Table 2 that the estimated percentage uncertainty was in the range of 0.06 and 4.23, and thus are within the acceptable range.

The multivariate linear regression model

The multivariate linear regression model was performed on the drying parameters, energy, and exergy parameters to develop or establish a mathematical relationship between the parameters and the drying process conditions (drying air temperature, drying air velocity, and relative humidity) as expressed in Eq. (40):

$$Y = b_o + b_1X_1 + b_2X_2 + b_3X_3 + \mu \tag{40}$$

Analysis of data

SPSS Statistics 15.0 (SPSS Inc., Chicago, IL, USA) software was utilized to fit the data to the multivariate linear regression model and to perform a one-way analysis of variance (ANOVA) in analyzing the effects of the drying process conditions on the studied parameters. Duncan's multiple range test at $P<0.05$ significance level and Least Significance Difference (LSD) was employed to examine the differences among mean or average values.

RESULTS AND DISCUSSION

Drying kinetics and drying parameters of red chili pepper

The drying kinetics of chili pepper drying are illustrated in Fig. 4 as plots of moisture ratio versus drying times at different drying air velocities, temperatures, and levels of relative humidity.

Fig. 4 shows that drying time varied at the different drying process conditions, indicating that the drying process is majorly determined through the process of diffusion [44]. The moisture ratio significantly ($P<0.05$) decreased with increasing drying time as the drying air temperature (Fig. 4(A)) and air velocity (Fig. 4(B)) increased as well as increased significantly with increasing relative humidity ((Fig. 4(C)). It is observed that

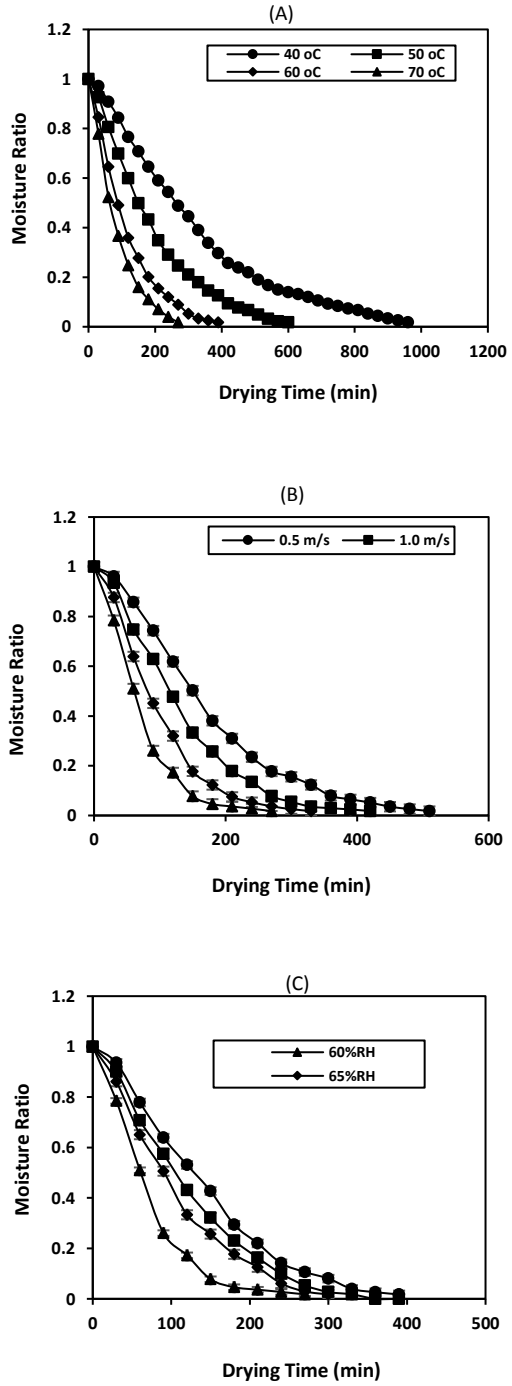

Fig. 4. (A) Drying curves for the variation of moisture ratio with drying air temperature at a constant air velocity of 2 m/s and 60% relative humidity (B) Drying curves for the variation of moisture ratio with drying air velocity at a constant air temperature of 70 ºC and 60% relative humidity. (C) Drying curves for the variation of moisture ratio with relative humidity at a constant air temperature of 70 ºC and air velocity of 2 m/s. The error bars indicate the standard deviation.

the drying time to obtain a dried chili pepper with constant weight (i.e. of 10.6% moisture content (wet basis)) at the different drying air temperatures: 40, 50, 60, and 70 ºC; drying air velocities: 0.5, 1.0, 1.5, and 2.0 m/s; and levels of relative humidity: 60, 65, 70, and 75% were found to be 960, 600, 390, and 270 min; 510, 420, 330, and 270 min; and 270, 300, 330, and 390 min, respectively. These observations indicate that drying time reduces as the respective drying air temperature and drying air velocity increase, and the relative humidity decreases. Similar observations of a decline in the drying time for an increase in drying air temperature have been reported for the drying of okra [58], red pepper, and bitter leaf [36]. Also, a decrease in drying time as a result of an increased drying air velocity has been reported for savory leaves [48], and kiwi [59] as well as for a decrease in relative humidity for the drying of pushkarmool (*Inula racemosa*) [44], and savory leaves [48].

The drying of chili pepper took place during the period of falling rate (plot not shown) at varying drying air temperatures, drying air velocities, and relative humidity, respectively. The multivariate linear regression model equation fitted to the drying data resulted in the following empirical equation expressed as follows:

$$\text{Drying Time} = 1432 - 18.06T - 176.9V + 740RH \quad R^2 = 0.992; \text{Adjusted } R^2 = 0.989 \tag{41}$$

Where T = air temperature, V = air velocity, and RH= relative humidity.

The model was found to be highly significant (P<0.05) with a high coefficient of determination (R^2) value of 0.992 and adjusted R^2 of 0.989 and thus adequate to predict the drying time for the chili pepper drying process. The effects of drying air temperature, drying air velocity, and relative humidity on the drying time were found to be highly significant (p<0.05). It is evident from the empirical equation that drying air temperature and drying air velocity had negative effects on the drying time, while relative humidity had a positive effect. This indicates that when drying air temperature and drying air velocity are respectively increased and relative humidity is step-down (or decreased), there is a decrease or reduction in the drying time.

The values of the drying parameters (drying coefficient, S and lag factor, G) obtained from the application of the moisture ratio equation (Eq. (9)) are provided in Table 3.

Table 3: Experimental conditions, drying parameters, and moisture transport parameters obtained from mass transfer models I to V for the slab-shaped chili pepper products.

Drying Conditions			Drying Parameters		Mass Transfer Model I (Dincer-Dost)				Mass Transfer Model II (Bi-Di Correlation)					Mass Transfer Model III (Bi-Re Correlation)				
T(℃)	V (m/s)	RH(%)	G	$S\times10^{4}$ (s^{-1})	Bi	μ_1	$D_{eff}\times10^{8}$(m^2/s)	$K_m\times10^{6}$ (m/s)	Di	Bi	μ_1	$D_{eff}\times10^{8}$(m^2/s)	$K_m\times10^{7}$ (m/s)	Re	Bi	μ_1	$D_{eff}\times10^{8}$(m^2/s)	$K_m\times10^{7}$ (m/s)
40	2.0	60	1.111	0.531	0.925	0.7712	2.01	1.24	2509095.47	0.1000	0.869	1.58	1.05	1828.72	0.2682	0.869	1.58	2.83
50	2.0	60	1.124	0.924	1.114	0.8298	3.02	2.24	1443001.44	0.1218	0.911	2.50	2.03	1779.48	0.2726	0.911	2.50	4.54
60	2.0	60	1.137	1.59	1.336	0.8902	4.51	4.02	838574.42	0.1493	0.952	3.94	3.92	1725.39	0.2776	0.952	3.94	7.29
70	2.0	60	1.156	2.18	1.741	0.9810	5.10	5.92	611620.80	0.1680	1.014	4.77	5.34	1680	0.2820	1.014	4.77	8.97
70	0.5	60	1.178	1.24	2.379	1.087	2.36	3.81	268817.20	0.2287	1.091	2.34	3.57	420	0.6389	1.091	2.34	9.97
70	1.0	60	1.171	1.61	2.152	1.053	3.27	4.74	414078.67	0.1945	1.066	3.19	4.14	840	0.4244	1.066	3.19	9.03
70	1.5	60	1.162	1.90	1.891	1.009	4.20	5.34	526315.79	0.1778	1.034	4.00	4.74	1260	0.3341	1.034	4.00	8.91
70	2.0	60	1.156	2.18	1.741	0.9810	5.10	5.92	611620.80	0.1680	1.014	4.77	5.34	1680	0.2820	1.014	4.77	8.97
70	2.0	60	1.156	2.18	1.741	0.9810	5.10	5.92	611620.80	0.1680	1.014	4.77	5.34	1680	0.2820	1.014	4.77	8.97
70	2.0	65	1.162	1.81	1.891	1.009	4.00	5.04	736648.25	0.1567	1.034	3.81	3.98	1698.46	0.2802	1.034	3.81	7.12
70	2.0	70	1.172	1.63	2.181	1.058	3.28	4.77	817995.91	0.1507	1.069	3.21	3.22	1712.31	0.2788	1.069	3.21	5.97
70	2.0	75	1.183	1.36	2.565	1.111	2.48	4.24	980392.16	0.1408	1.110	2.48	2.33	1724.62	0.2776	1.110	2.48	4.59

Table 3: Experimental conditions, drying parameters, and moisture transport parameters obtained from mass transfer models I to V for the slab-shaped chili pepper products. (Continuation)

Drying Conditions			Drying Parameters		Mass Transfer Model IV (Bi-S Correlation)				Mass Transfer Model V (Bi-G Correlation)			
T (°C)	V (m/s)	RH (%)	G	$Sx10^{-4}$ (s^{-1})	Bi	μ_1	$D_{eff} \times 10^{-8}$ (m^2/s)	$K_m \times 10^{-7}$ (m/s)	Bi	μ_1	$D_{eff} \times 10^{-8}$ (m^2/s)	$K_m \times 10^{-6}$ (m/s)
40	2.0	60	1.111	0.531	0.050	0.869	1.58	0.53	0.957	0.869	1.58	1.01
50	2.0	60	1.124	0.924	0.056	0.911	2.50	0.93	1.306	0.911	2.50	2.18
60	2.0	60	1.137	1.59	0.067	0.952	3.94	1.76	1.775	0.952	3.94	4.63
70	2.0	60	1.156	2.18	0.075	1.014	4.77	2.39	2.763	1.014	4.77	8.79
70	0.5	60	1.178	1.24	0.062	1.091	2.34	0.97	4.571	1.091	2.34	7.13
70	1.0	60	1.171	1.61	0.068	1.066	3.19	1.45	3.898	1.066	3.19	8.29
70	1.5	60	1.162	1.90	0.071	1.034	4.00	1.89	3.173	1.034	4.00	8.46
70	2.0	60	1.156	2.18	0.075	1.014	4.77	2.39	2.763	1.014	4.77	8.79
70	2.0	60	1.156	2.18	0.075	1.014	4.77	2.39	2.763	1.014	4.77	8.79
70	2.0	65	1.162	1.81	0.070	1.034	3.81	1.78	3.173	1.034	3.81	8.06
70	2.0	70	1.172	1.63	0.068	1.069	3.21	1.46	3.988	1.069	3.21	8.53
70	2.0	75	1.183	1.36	0.064	1.110	2.48	1.06	5.118	1.110	2.48	8.46

As it can be seen in Table 3, the drying coefficients (S) increased with increasing velocity and temperature of the drying air medium. However, they decreased with increasing relative humidity. The lag factor increases with increasing velocity, relative humidity, and temperature of the drying air medium. The estimated values of the lag factor were found to be greater than 1 and they ranged from 1.111 to 1.180 under all the varying drying process conditions, thus indicating the occurrence of an increased drying rate period [24]. A multivariate linear regression model equation was fitted to the S and G data, respectively. The model fit was found to be highly significant (P<0.05) with high R^2 values of 0.991 for S and 0.988 for G. The empirical equations obtained from the fittings are expressed as follows:

$$S = 2.89\times10^{-5} + 5.68\times10^{-6}\,T + 5.91\times10^{-5}\,V - 5.50\times10^{-4}\,RH \quad R^2 = 0.991 \tag{42a}$$

$$G = 0.97 + 1.50\times10^{-3}\,T - 0.016\,V + 0.181\,RH \quad R^2 = 0.996$$

Variance analysis revealed that the effects of drying air temperature, velocity, and relative humidity on the drying coefficient and lag factor were highly significant (P<0.05). Therefore, by substituting Eq. (42a) into Eq. (9), the moisture content distribution can be obtained as:

$$MR = 0.97 + 0.00150\,T - 0.016\,V + 0.181\,RH)\exp(-[2.89\times10^{-5} + 5.67\times10^{-6}\,T + 5.91\times10^{-5}\,V - 5.50\times10^{-4}\,RH]\times t) \tag{42b}$$

The predicted or theoretical values of S and G are presented in Table 2. From Table 2, it is observed that there is a high agreement between the measured and theoretical values as depicted by the very low values of the percentage errors.

Mass transfer parameters: Moisture diffusivity and mass transfer coefficients

The values of the mass transfer parameters (Biot number, Bi, the root of the characteristic equation, μ_1, effective moisture diffusivity, D_{eff}, and mass transfer coefficient, K_m) obtained from the application of the mass transfer model equations are provided in Table 3. The calculated Biot numbers were obtained using the five different

mass transfer model equations for all the drying process conditions ranged from 0.050 to 5.118. These values are generally greater than 0.050, which confirms the earlier presumption that there are internal and external resistances to moisture diffusion in the chili pepper. Meanwhile, if the value of Biot number is greater than 30, the drying process is completely diffusion-controlled [24, 60]. The results in Table 3 showed that with mass transfer models I, II, III, IV, and V, the Biot numbers were influenced by the drying air velocity, the relative humidity, and the drying air temperature. It was observed that the Biot number values estimated with the mass transfer models I and V generally increase with the increase in the drying air temperature and relative humidity while it decreases with an increase in drying air velocity. The Biot numbers calculated with the mass transfer models II and III increased with increasing drying air temperature and decreased with increasing relative humidity and drying air velocity. Also, the values of the Biot number estimated with the mass transfer model IV increased with increasing drying air velocity and temperature and decreased with increasing relative humidity. A similar trend of results under the drying conditions of air velocity and the temperature has been reported for slab potato slices [17]. However, *Ju et al.* [24] have reported an increasing Biot number due to increasing relative humidity using the *Bi - Di* correlation.

The values of the effective moisture diffusivity and the mass transfer coefficient of the chili pepper samples varied with the varying drying process conditions. The values of the effective moisture diffusivity were found to range from 2.36-5.10×10^{-8} m^2/s, 5.10-2.48×10^{-8} m^2/s, and 2.01-5.10×10^{-8} m^2/s according to mass transfer model I for drying air velocity, relative humidity, and drying air temperature, respectively. Also, according to the mass transfer models II to V, the effective moisture diffusivity values range from 2.34-4.77×10^{-8} m^2/s, 4.77-2.48×10^{-8} m^2/s, and 1.58-4.77×10^{-8} m^2/s for drying air velocity, relative humidity, and drying air temperature, respectively. These calculated values indicate that effective moisture diffusivity increases with increasing drying air velocity and temperature while it declines with increasing relative humidity. A rise in the temperature decreases the viscosity of moisture and subsequently the moisture diffusion resistance. This results in facilitating moisture diffusion in the food material capillaries and thus leading to increased moisture diffusivity [23]. This increase in effective moisture diffusivity observed in this study is similar to the observations that have been reported of an increase in diffusivity coefficient due to an increased drying air temperature [23, 25, 36, 44, 61, 62] and drying air velocity [21, 61], and a decrease in relative humidity [44, 48, 62]. However, *Abbaszadeh et al.* [25] have reported a decrease in effective moisture diffusivity due to increased air velocity in the hot air drying of Russian olive fruit. The values obtained at the different drying process conditions are within 10^{-12} to 10^{-8} m^2/s range that has generally been obtained by various workers for the drying of food materials [61].

The values of the mass transfer coefficient were found to range from 3.81-5.92×10^{-6} m/s 5.92-4.24×10^{-6} m/s, and 1.24-5.92×10^{-6} m/s according to mass transfer model I for drying air velocity, relative humidity, and drying air temperature, respectively. Also, according to moisture transfer model II, the mass transfer coefficient values ranged from 3.57-5.34×10^{-7} m/s, 5.34-2.33×10^{-7} m/s, and 1.05-5.34×10^{-7} m/s for drying air velocity, relative humidity, and drying air temperature, respectively; it ranged from 9.97-8.97×10^{-7} m/s, 8.97-4.59×10^{-7} m/s, and 2.83-8.97×10^{-7} m/s for drying air velocity, relative humidity, and drying air temperature, respectively according to mass transfer model III while it ranged from 0.97-2.39×10^{-7} m/s, 2.39-1.06×10^{-7} m/s, and 0.53-2.39×10^{-7} m/s for drying air velocity, relative humidity, and drying air temperature respectively according to mass transfer model IV as well as from 7.13-8.79×10^{-6} m/s, 8.79-8.46×10^{-6} m/s, and 1.01-8.79×10^{-6} m/s respectively based on mass transfer model V. The results showed that using mass transfer models I, II, IV, and V, the mass transfer coefficient generally increases with increasing drying air velocity and temperature while it declines with increasing relative humidity. However, with the use of mass transfer model III the estimated mass transfer coefficient was observed to decrease with increasing drying air velocity. This may probably be due to the rising air turbulence (laminar flow of air) as drying air velocity increases.

Prediction of theoretical moisture ratio, mass transfer parameters, half-drying times, and their validation

Predicted or calculated moisture ratios obtained at different temperatures of 40-70 °C, air velocities (0.5-2.0 m/s), and levels of relative humidity (60-75%) from moisture transfer models I-V and the multivariate linear

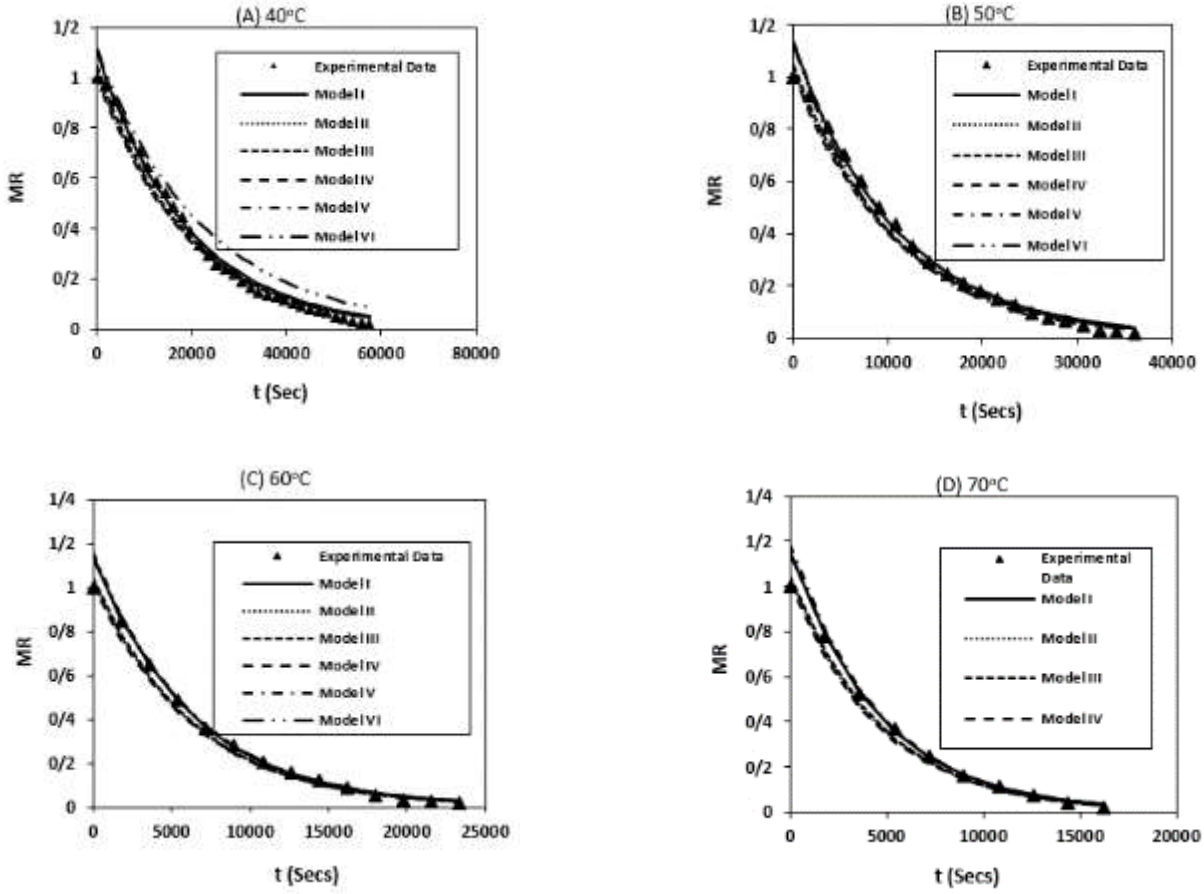

Fig. 5: Comparison between the experimental moisture ratio and the predicted or calculated moisture ratio obtained from the six models considered at a constant air velocity of 2 m/s and relative humidity of 60% but at different drying air temperatures of (A) 40°C, (B) 50°C, (C) 60°C, and (D) 70°C.

regression model equation (Eq. 37b) (model VI) were compared with the experimental moisture ratio (i.e. normalized moisture content) as illustrated in Figs. 5 - 7.

It can be seen in Figs. 5 - 7 that the calculated or theoretical and experimental moisture ratio profiles exponentially decrease with increasing drying time and the theoretical moisture ratios obtained from the application of the five models adequately agree well with the experimental moisture ratios as validated by the high modeling efficiency (R^2) values greater than 0.95 (Table 4).

That is, the statistical data (R^2 and RMSE) in Table 4 showed that all the five mass transfer models (model I-V) and the multi-linear regression model (model VI) gave an adequate fit as demonstrated by the relatively high R^2 values (> 0.90) and very low RMSE values (< 0.005). This implies that all six models can be used to predict the moisture content distribution during the drying of food products. Nevertheless, the RMSE values for models V and VI are relatively lower than the values for other mass transfer models. Thus, models V and VI serve as the most adequate models to be applied for the prediction of mass transfer parameters in the course of convective cabinet hot air drying of chili pepper. However, the corrected Akaike Information Criterion (AIC_C) was used as the criterion to verify the conclusion drawn from the RMSE error function analysis and to select the best model as well as to rank the rest of the models. Based on AIC_C, model VI has the average minimum AIC_C value of 65.03 and thus suggests that the predicted or calculated data obtained from this model fits the experimental values better than the other five mass transfer model equations. The model equations ranking was performed based on the calculated values of the Relative Akaike Weight (λ_A) (Table 4). The values evidently distinguish the appropriateness of the six model equations ranking model VI (multi-linear regression model) as the first (λ_A= 1.00),

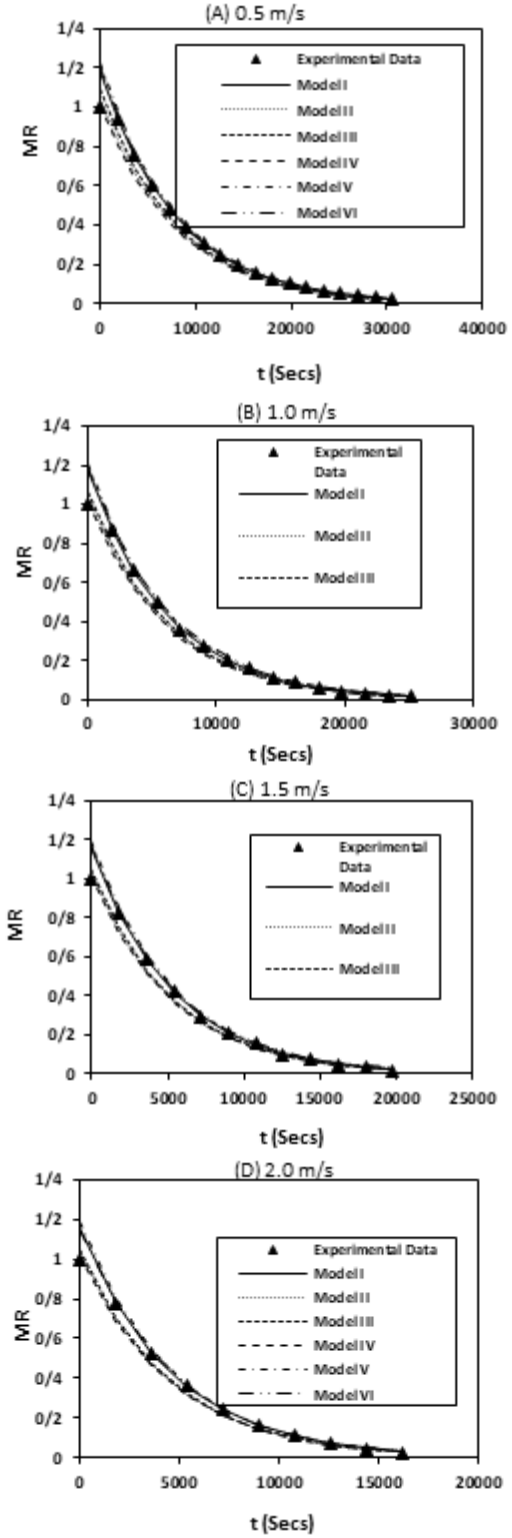

Fig. 6. Comparison between the experimental moisture ratio and the predicted or calculated moisture ratio obtained from the six models considered at a constant drying air temperature of 70 °C and relative humidity of 60% but at different drying air velocities of (A) 0.5 m/s, (B) 1.0 m/s, (C) 1.5 m/s, and (D) 2.0 m/s.

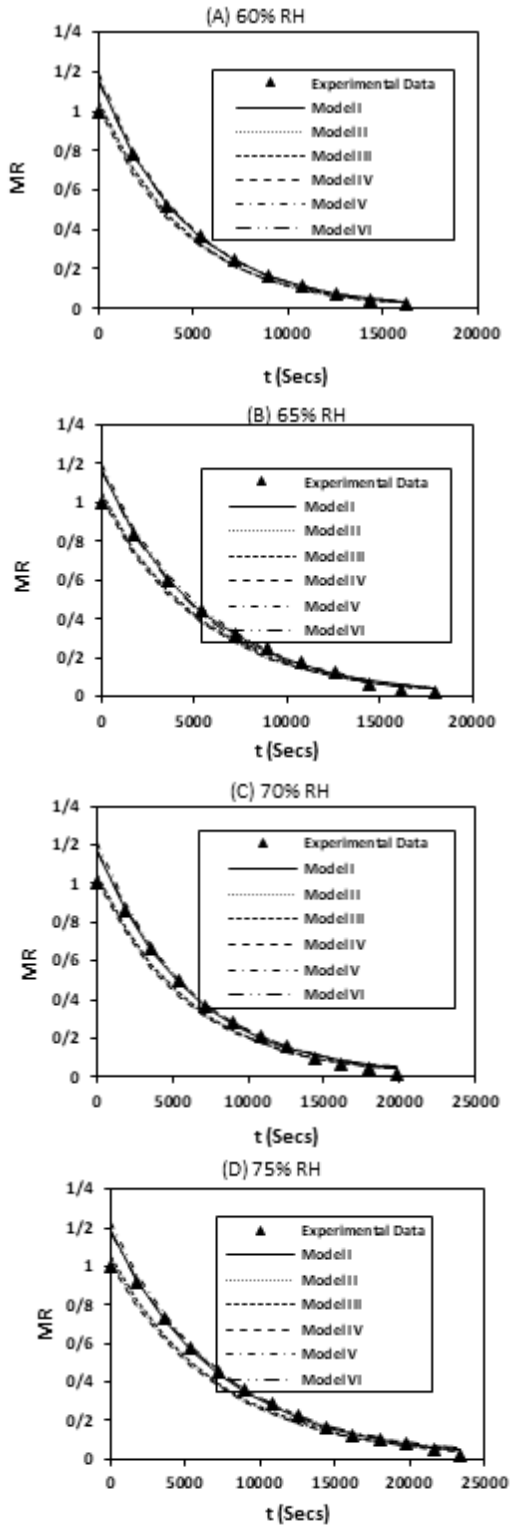

Fig. 7: Comparison between the experimental moisture ratio and the predicted or calculated moisture ratio obtained from the six models considered at a constant drying air temperature of 70 °C and air velocity of 2.0 m/s but at different levels of relative humidity of (A) 60%, (B) 65%, (C) 70%, and (D) 75%.

Table 4: Results of the Error Analysis.

Drying Conditions			Modelling Efficiency (R^2)					
T (°C)	V (m/s)	RH (%)	Model I	Model II	Model III	Model IV	Model V	Model VI
40	2	60	0.993	0.993	0.993	0.993	0.993	0.996
50	2	60	0.992	0.992	0.992	0.992	0.992	0.986
60	2	60	0.992	0.992	0.992	0.992	0.992	0.992
70	2	60	0.990	0.990	0.990	0.990	0.990	0.991
70	0.5	60	0.990	0.990	0.985	0.990	0.990	0.984
70	1.0	60	0.990	0.990	0.988	0.990	0.990	0.990
70	1.5	60	0.990	0.990	0.989	0.990	0.990	0.991
70	2.0	60	0.990	0.990	0.990	0.990	0.990	0.991
70	2.0	60	0.990	0.990	0.990	0.990	0.990	0.991
70	2.0	65	0.986	0.986	0.986	0.986	0.986	0.983
70	2.0	70	0.985	0.985	0.985	0.985	0.985	0.986
70	2.0	75	0.985	0.984	0.984	0.984	0.985	0.987
Drying Conditions			Root Mean Square Error (RMSE)					
T (°C)	V (m/s)	RH (%)	Model I	Model II	Model III	Model IV	Model V	Model VI
40	2	60	0.0034	0.0030	0.0034	0.0018	0.0011	0.0018
50	2	60	0.0017	0.0015	0.0019	0.0017	0.0010	0.0014
60	2	60	0.0015	0.0014	0.0020	0.0015	0.0010	0.0012
70	2	60	0.0026	0.0024	0.0026	0.0018	0.0013	0.0010
70	0.5	60	0.0025	0.0024	0.0028	0.0038	0.0019	0.0013
70	1.0	60	0.0027	0.0024	0.0029	0.0026	0.0015	0.0011
70	1.5	60	0.0025	0.0025	0.0027	0.0020	0.0014	0.0012
70	2.0	60	0.0026	0.0024	0.0028	0.0018	0.0013	0.0010
70	2.0	60	0.0026	0.0024	0.0028	0.0018	0.0013	0.0010
70	2.0	65	0.0030	0.0028	0.0033	0.0025	0.0018	0.0015
70	2.0	70	0.0029	0.0028	0.0031	0.0029	0.0021	0.0018
70	2.0	75	0.0027	0.0026	0.0030	0.0036	0.0026	0.0024
Drying Conditions			Corrected Akaike Information Criterion (AIC_C)					
T (°C)	V (m/s)	RH (%)	Model I	Model II	Model III	Model IV	Model V	Model VI
40	2	60	201.87	186.57	197.46	182.56	201.27	151.91
50	2	60	117.06	110.00	115.68	107.19	114.54	109.24
60	2	60	65.26	66.74	69.06	64.72	62.40	65.21
70	2	60	36.35	39.45	40.34	38.43	34.01	36.70
70	0.5	60	87.94	86.16	86.87	81.78	81.50	83.90
70	1.0	60	67.90	67.57	70.66	66.91	63.65	64.54
70	1.5	60	48.89	51.63	52.64	49.96	45.38	47.96
70	2.0	60	36.35	39.45	40.34	38.43	34.01	36.70
70	2.0	60	36.35	39.45	40.34	38.43	34.01	36.70
70	2.0	65	41.59	43.17	44.37	42.09	38.87	41.36
70	2.0	70	47.24	47.73	49.23	46.55	43.97	47.04
70	2.0	75	58.83	57.11	59.21	55.72	54.48	59.07
			$\lambda_A = 15.18$	$\lambda_A = 9.78$	$\lambda_A = 35.69$	$\lambda_A = 3.86$	$\lambda_A = 3.17$	$\lambda_A = 1.00$

Table 5: Experimental conditions, theoretical drying parameters, and theoretical moisture transport parameters obtained from mass transfer models for dried chili products.

Drying Conditions			Predicted Drying Parameters Using Model VI		Predicted Mass Transfer Parameters Obtained Using Model VI in Conjunction with Mass Transfer Model IV (Bi-S Correlation)				Predicted Mass Transfer Parameters Obtained Using Model VI in Conjunction with Mass Transfer Model V (Bi-G Correlation)			
T (°C)	V (m/s)	RH (%)	G	$Sx10^{-4}$ (s^{-1})	Bi	μ_t	$D_{eff} \times 10^{-8}$ (m^2/s)	$K_m \times 10^{-7}$ (m/s)	Bi	μ_t	$D_{eff} \times 10^{-8}$ (m^2/s)	$K_m \times 10^{-6}$ (m/s)
40	2.0	60	1.107	0.443	0.044	0.8551	1.35 (16.2%)	0.40 (32.5%)	0.8693	0.8551	1.35 (16.2%)	0.78 (29.5%)
50	2.0	60	1.122	1.01	0.058	0.9047	2.78 (-13.1%)	1.07 (-13.1%)	1.245	0.9047	2.78 (-13.1%)	2.31 (-5.63%)
60	2.0	60	1.137	1.58	0.067	0.9524	3.92 (0.51%)	1.75 (0.57%)	1.775	0.9524	3.92 (0.51%)	4.64 (-0.22%)
70	2.0	60	1.152	2.15	0.074	1.001	4.83 (-1.24%)	2.38 (0.42%)	2.519	1.001	4.83 (-1.24%)	8.11 (8.38%)
70	0.5	60	1.176	1.26	0.062	1.084	2.41 (-2.90%)	1.00 (-3.00%)	4.368	1.084	2.41 (-2.90%)	7.02 (1.57%)
70	1.0	60	1.168	1.56	0.067	1.055	3.15 (1.27%)	1.41 (2.84%)	3.640	1.055	3.15 (1.27%)	7.64 (8.51%)
70	1.5	60	1.160	1.86	0.071	1.027	3.97 (0.76%)	1.88 (0.53%)	3.030	1.027	3.97 (0.76%)	8.02 (5.49%)
70	2.0	60	1.152	2.15	0.074	1.001	4.83 (-1.24%)	2.38 (0.42%)	2.519	1.001	4.83 (-1.24%)	8.11 (8.38%)
70	2.0	60	1.152	2.15	0.074	1.001	4.83 (-1.24%)	2.38 (0.42%)	2.519	1.001	4.83 (-1.24%)	8.11 (8.38%)
70	2.0	65	1.161	1.87	0.071	1.031	3.96 (-3.79%)	1.87 (-5.06%)	3.101	1.031	3.96 (-3.79%)	8.19 (-1.59%)
70	2.0	70	1.170	1.60	0.067	1.062	3.19 (0.63%)	1.42 (2.82%)	3.811	1.062	3.19 (0.63%)	8.10 (5.31%)
70	2.0	75	1.179	1.32	0.063	1.095	2.48 (0.00%)	1.04 (1.92%)	4.676	1.095	2.48 (0.00%)	7.73 (9.44%)

N.B: The values in the bracket represent the percentage difference between calculated D_{eff} from experimental data and theoretical/predicted D_{eff} as well as the percentage difference between calculated K_m and theoretical K_m .

model V (Bi-G) with λ_A, 3.17 as the second, and model IV (Bi-S) with λ_A, 3.86 as the third best model equation to fit the experimental data. Thus, the predicted S and G values obtained using model VI were applied to models IV and V to obtain predicted or theoretical effective moisture diffusivities and mass transfer coefficients (Table 5). The differences between the experimental effective moisture diffusivity and theoretical effective moisture diffusivities as well as the differences between the measured or calculated mass transfer coefficient and the predicted or theoretical mass transfer coefficients are also provided in Table 5.

From Table 5, it is generally seen that there is a high agreement between the measured and theoretical effective moisture diffusivities as well as between the measured mass transfer coefficients and theoretical mass transfer coefficients. This implies that model VI can be utilized in conjunction with the moisture transfer models to predict moisture transfer parameters. Also, it can be observed from Figs. 5 - 7 and Table 3 that the regression moisture ratio value at t = 0 is more than 1 for each of the six models. Nonetheless, this is expected due to the nature of moisture diffusion, giving rise to the lag factor. As seen in Table 3, all the lag factors are greater than 1, revealing that there is a kind of internal resistance to the diffusion of moisture in the sample.

Furthermore, the experimental and predicted or theoretical half-drying times of chili pepper were investigated. Half-drying time is defined as the time required to decrease the difference in product moisture content between the product and the drying medium by one-half. Therefore, substituting MR = 0.5 into Eq. (9), the Half-Drying Time (HDT) becomes [17]:

$$HDT = \frac{\ln 2G}{S} \tag{43}$$

Using Eq. (43) with the predicted and measured experimental moisture content values, the determined half-drying times for chili pepper are presented in Table 6. The differences that exist between the experimental half-drying times and the predicted or theoretical drying times are also listed in Table 6. Thus, the experimentally measured half-drying times when compared with the predicted half-drying times on the basis of their differences showed that in general, there is a high agreement between the experimental and predicted half-drying times except for cases of models II, III, and IV, respectively.

Table 6. The experimental and predicted or theoretical half-drying time and their comparison.

Drying Conditions			Experimental	Model I	Model II	Model III	Model IV	Model V	Model VI
T (°C)	V (m/s)	RH (%)	15800	15025 (5.16%)	13383 (18.06%)	13860 (14%)	13212 (19.59%)	15059 (4.92%)	17881 (-11.64%)
40	2.0	60							
50	2.0	60	8978	8767 (2.41%)	7737 (16.04%)	7977 (12.55%)	7631 (17.65%)	8872 (1.19%)	8003 (12.18%)
60	2.0	60	5284	4957 (6.60%)	4523 (16.83%)	4640 (13.88%)	4434 (19.17%)	5277 (0.13%)	5200 (1.62%)
70	2.0	60	3862	3845 (0.44%)	3313 (16.57%)	3387 (14.02%)	3243 (19.09%)	3970 (-2.72%)	3878 (-0.41%)
70	0.5	60	7200	6911 (4.18%)	5898 (22.08%)	6213 (15.89%)	5686 (26.63%)	7180 (0.28%)	6788 (6.07%)
70	1.0	60	5400	5286 (2.16%)	4513 (19.65%)	4692 (15.09%)	4385 (23.15%)	5484 (-1.53%)	5439 (-0.72%)
70	1.5	60	4559	4438 (2.73%)	3809 (19.69%)	3906 (16.72%)	3716 (22.69%)	4595 (-0.78%)	4525 (0.75%)
70	2.0	60	3862	3845 (0.44%)	3313 (16.57%)	3387 (14.02%)	3243 (19.09%)	3970 (-2.72%)	3878 (-0.41%)
70	2.0	60	3862	3845 (0.44%)	3313 (16.57%)	3387 (14.02%)	3243 (19.09%)	3970 (-2.72%)	3878 (-0.41%)
70	2.0	65	4777	4659 (2.53%)	3980 (20.03%)	4078 (17.14%)	3901 (22.46%)	4823 (-0.95%)	4510 (5.92%)
70	2.0	70	5400	5226 (3.33%)	4414 (22.34%)	4523 (19.39%)	4330 (24.64%)	5422 (-0.41%)	5329 (1.33%)
70	2.0	75	6479	6332 (2.32%)	5279 (22.73%)	5425 (19.43%)	5184 (24.98%)	6583 (-1.58%)	6499 (-0.31%)

N.B: T = Temperature; V = Velocity; RH = Relative humidity. The values in the bracket are the percentage difference between experimental data and model results

Energy analysis

Energy utilization ratio, total energy consumption, specific energy consumption, and heat loss

The calculated results for the EUR, TEC, SEC, and heat loss in the course of chili drying are depicted in Fig. 8 which revealed that EUR, energy consumption (TEC and SEC), and heat loss significantly (P<0.05) decreased with increasing drying air temperature (Fig. 8(A-B)) while it increased significantly (P<0.05) with increasing relative humidity (Fig. 8(C-D)) and drying air velocity (Fig. 8(E-F)). Also, since there is a direct relationship between energy consumption and Energy Utilization (EU), thus it implies that EU decreases as drying air temperature increases as well as increases as relative humidity and drying air velocity respectively increase.

At varying drying air velocities (0.5-2.0 m/s), relative humidity (60-75%), and drying air temperatures (40-70 °C), the values of EUR were obtained to be in the range of 0.035-0.137, 0.137-0.175, and 0.325-0.137, TEC values were found to be in the range of 43.56-52.57 MJ; 52.57-77.36 MJ; and 62.40-52.57 MJ, SEC values were obtained to be in the range of 49.0-59.13 MJ; 59.13-87.02 MJ; and 70.19-59.13 MJ, while the values of heat loss varied from the range of 0.16 to 0.34 MJ; 0.34 to 0.52 MJ; and 2.39 to 0.34 MJ, respectively. Similar observations of decreasing energy consumption (TEC and SEC) due to an increment in drying air temperature have been reported for St John's Wort leaves [54], apple slices [20], onion slices [63], *inula racemosa* [44], and ginseng [62]. Similarly, increase in TEC due to increasing drying air velocity have been reported for the drying of St John's Wort leaves [54], apple slices [20], eggplant [64], and onion slices [63]; while *Agnihotri et al.* [44] and *Ju et al.* [62] have similarly reported an increasing SEC as relative humidity increases for the drying of *inula racemosa* and ginseng root, respectively. In addition, *Nazghelichi et al.* [34], *Kaveh et al.* [43], and *Mondal et al.* [42] have reported a similar observation of a decreasing EUR as a result of an increasing drying temperature for the drying of carrots in a fluidized bed dryer, pennyroyal leaves in a laboratory hybrid (solar-hot air) dryer, and grain in a mixed flow dryer, respectively.

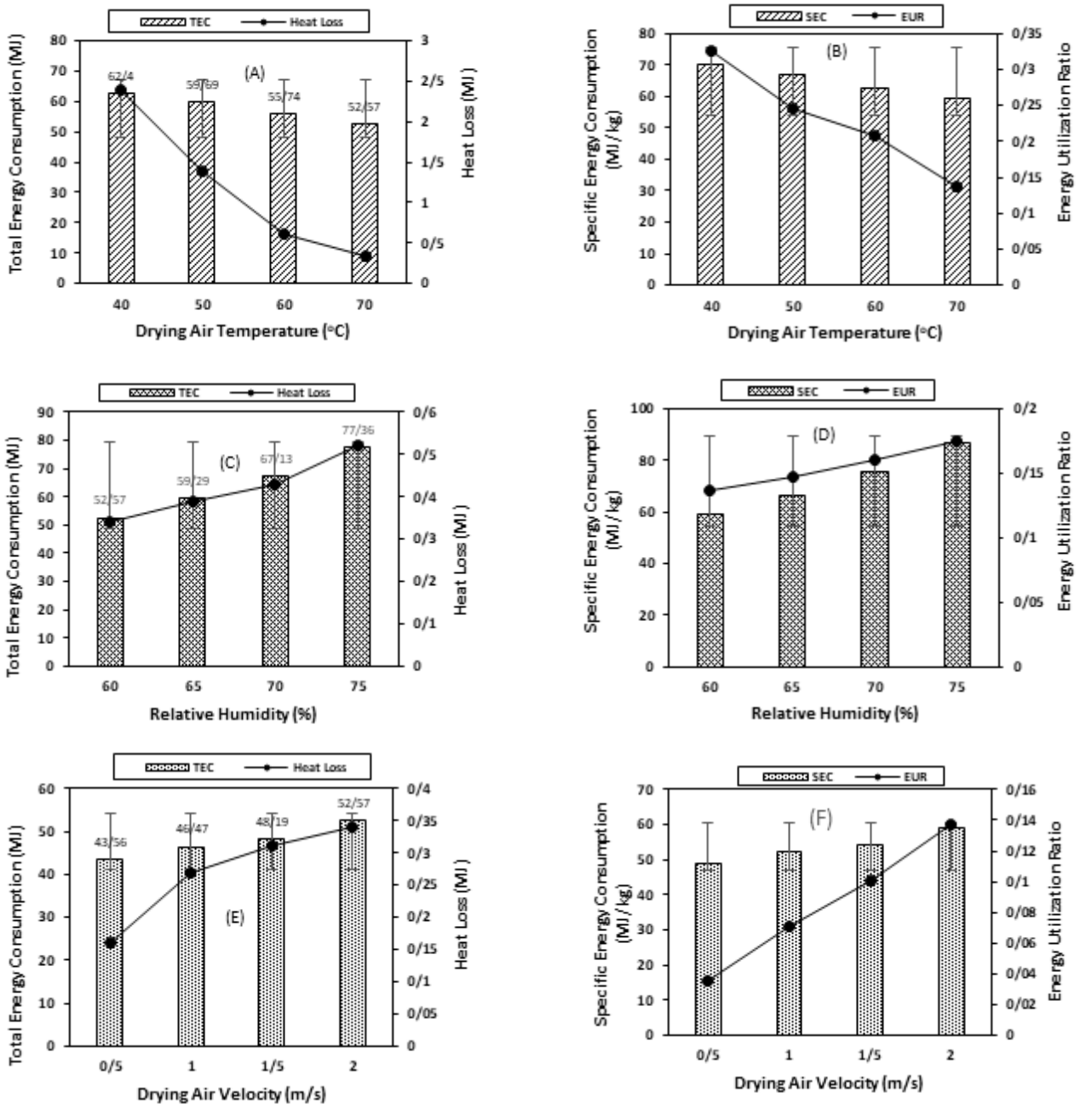

Fig. 8: (A) Total energy consumption and heat loss at different drying air temperatures. (B)) Specific energy consumption and energy utilization ratio at different drying air temperatures. (C) Total energy consumption and heat loss at different relative humidity. (D) Specific energy consumption and energy utilization ratio at different relative humidity. (E) Total energy consumption and heat loss at different drying air velocities. (F) Specific energy consumption and energy utilization ratio at different drying air velocities. The error bars indicate the standard deviation.

Also, an increase in EUR due to increasing air velocity has been observed and reported for the drying of pennyroyal leaves by *Kaveh et al.* [43]. A multivariate linear regression model equation fitted to the energy parameters (TEC and SEC) were found to be highly significant (P<0.05) with a high R^2 value of 0.995 and adjusted R^2 of 0.993. The empirical equations obtained from the fittings are expressed as follows:

Table 7: Values for the energy and drying efficiencies of chili pepper drying in a cabinet-tray dryer

Drying Condition	η_E (%)	η_D (%)
Air Velocity (m/s)		
0.5	4.78	5.17
1.0	4.48	4.84
1.5	4.32	4.50
2.0	3.96	4.12
Relative Humidity (%)		
60	3.96	4.12
65	3.51	3.66
70	3.10	3.23
75	2.69	2.80
Temperature (°C)		
40	3.42	3.45
50	3.55	3.62
60	3.77	3.88

$$TEC = -31.55 - 0.35T + 5.84V + 161.3RH \quad (44)$$

$$R^2 = 0.995; Adjusted\ R^2 = 0.993$$

$$SEC = -35.50 - 0.40T + 6.56V + 181.5RH$$

$$R^2 = 0.995; Adjusted\ R^2 = 0.993$$

Variance analysis revealed that the effects of drying air temperature, velocity, and relative humidity on energy consumption were highly significant (P<0.05). Furthermore,

Table 7 shows the values of energy efficiency (η_E) and drying efficiency (η_D) for the drying of chili pepper slices where both energy and dry efficiencies increased with declining drying air velocity, relative humidity, and increasing drying air temperature.

At varying drying air velocities (0.5-2.0 m/s), relative humidity (60-75%), and drying air temperatures (40-70 °C), η_E values were found to be in the range of 4.78-3.96%, 3.96-2.69%, and 3.42-3.96%, respectively, while η_D values were obtained to be in the range of5.17-4.12%, 4.12-2.80%, and 3.45-4.12%, respectively. The η_E values agreed well with the range of values of 1.91 to 10% that have been reported in the literature [20, 65] while the η_D values are within the range of values of 1.6 to 65% that have been published in the literature [19, 20, 66]. A similar observation of increased energy efficiency with rising drying air temperature and a declining air velocity has been reported by Beigi [20] for the convective hot air drying of apple slices.

The multivariate linear regression model equation fitted very well to the energy efficiency data which resulted in the following empirical equations expressed as follows:

$$\eta_E = 8.88 + 0.019T - 0.55V - 8.57RH \quad (45)$$

$$R^2 = 0.997; Adjusted\ R^2 = 0.996$$

$$\eta_D = 9.23 + 0.023T - 0.71V - 8.84RH \quad (46)$$

$$R^2 = 0.999; Adjusted\ R^2 = 0.999$$

The model equations were found to be highly significant (P < 0.05) with high R^2 values of 0.997, 0.999, and adjusted R^2 values of 0.996 and 0.999. Variance analysis showed that the effects of drying air temperature, velocity, and relative humidity on the energy and drying efficiencies were highly significant (P<0.05).

Exergy analysis

Fig. 9 illustrates the effects of drying air temperature, relative humidity and drying air velocity on the exergy rates and exergetic efficiencies of the chili pepper convective drying process.

It was observed that when the drying air temperature rose from 40-70 °C at a constant drying air velocity of 2 m/s and relative humidity of 60%, the exergy rates and the exergetic efficiencies respectively increased with values ranging from 0.181-2.875kW (exergy inflow rates), 0.155-2.673kW (exergy outflow rates), 0.026-0.202kW (exergy loss rates), and 85.6-93% (exergetic efficiencies) (Fig. 9(A)). Similar observations of increased exergy rates and exergetic efficiencies due to increased temperature have been reported for the convective tray drying of broccoli [67], column drying of walnut [57], and mixed flow drying of maize grain [42]. On the other hand, Erbay and Icier [27], *Castro et al.* [28], and *Folayan et al.* [33] have respectively reported decreased exergetic efficiencies due to increasing drying temperature for the convective tray drying of olive leaves and onion.

As presented in Fig. 9(B) which illustrates the variation of exergy inflow rates, exergy outflow rates, exergy loss

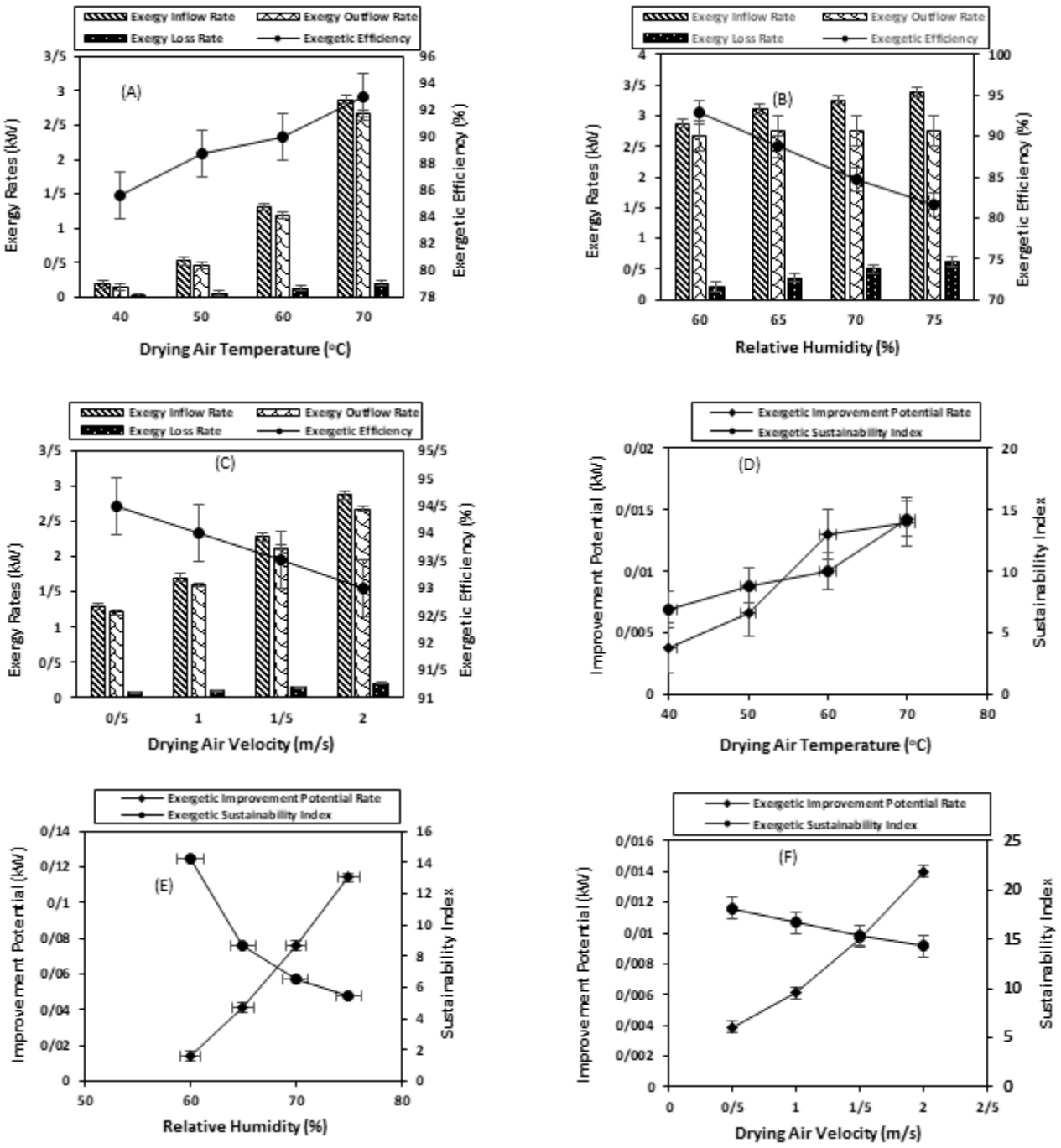

Fig. 9. (A)Variation of exergy rates and exergetic efficiency with drying air temperature. (B) Variation of exergy rates and exergetic efficiency with relative humidity. (C) Variation of exergy rates and exergetic efficiency with drying air velocity. (D) Variation of exergetic improvement potential rate and exergetic sustainability index with drying air temperature. (E) Variation of exergetic improvement potential rate and exergetic sustainability index with relative humidity. (F) Variation of exergetic improvement potential rate and exergetic sustainability index with drying air velocity. The error bars indicate the standard deviation.

rates and exergetic efficiencies with relative humidity, it was seen that as the relative humidity changed from 60-75% so also the exergy rates changed with the exergy inflow, exergy outflow, and exergy loss rates increasing from 2.875-3.376 kW, 2.673-2.760 kW, and 0.202-0.622 kW, respectively, while the exergetic efficiencies

decreasing from 93%-81.6%. This observation of decreasing energetic efficiencies due to increasing relative humidity is in concordance with the report of *Dincer* and *Sahin* [45]. For the drying air velocity in the range of 0.5–2.0 m/s (Fig. 9(C)), the exergy rates varied from 1.286-2.875 kW (exergy inflow), 1.215-2.673 kW (exergy outflow), and 0.071-0.202 kW (exergy loss), respectively, while the energetic efficiencies slightly varied from 94.5 to 93%. Thus, the results indicate that exergy rates (exergy inflow, outflow, and exergy loss) increased with increasing drying air velocity, while exergetic efficiencies decreased with increasing drying air velocity. A similar observation has been reported for the mixed flow drying of maize grain [42]. Concerning exergetic efficiency, *Castro et al.* [28] have reported a decrease in exergetic efficiency due to increasing drying air velocity in the convective tray drying of onions.

The exergetic efficiency values obtained in this study for the convective hot air drying of chili pepper using a cabinet-tray dryer varied from 73 to 94.5% over the drying air velocities, drying air temperatures, and different levels of relative humidity. Exergetic efficiency values that range from 3 to 100% have been reported in the literature for the drying of other agricultural products using different drying equipment [27, 28, 34, 42, 57, 64]. A multivariate linear regression model equation fitted well to the exergetic efficiencies data and was found to be highly significant (P<0.05) with a high R^2 value of 0.994 and adjusted R^2 value of 0.992. The empirical equation obtained from the fitting is expressed as follows:

$$\eta_{Ex} = 125.3 + 0.23T - 1.14V - 77.6RH \quad (47)$$

$$R^2 = 0.994; \quad Adj\ R^2 = 0.992$$

Variance analysis showed that the effects of drying air temperature, drying air velocity, and relative humidity on the exergetic efficiency were highly significant (P<0.05).

To achieve the Exergetic Improvement Potential (EIP) of the cabinet-tray dryer, EIP values at different drying air velocities, drying air temperature, and relative humidity was calculated and the results are presented in Fig. 9(D) – (F). At the drying air temperature range (40-70 ^oC), relative humidity range (60-75%), and drying air velocity range (0.5-2.0 m/s), the EIP values correspondingly varied from 0.0038-0.014 kW; 0.014-0.114 kW; and 0.0087-0.014 kW. The results indicate that EIP values generally increased with increasing drying air temperature and relative humidity, while it decreased with a rise in drying air velocity. The EIP increased 3.68 times as the temperature was increased from 40-70 °C indicating that the cabinet-tray drying chamber insulation should further be improved for increased or higher performance, especially at higher temperatures. An observation of increasing EIP due to an increase in temperature has been reported for convective hot air drying of olive leaves [27], onion [28], and maize grain [42], while an increase of EIP with rising air velocity has been published by *Icier et al.* [67] and Erbay and Icier [27] for broccoli and olive leaves, respectively. The EIP as a function of drying air temperature, drying air velocity, and relative humidity was appropriately modeled with a multivariate linear regression model equation as expressed in Eq. (48):

$$EIP = -0.40 + 3.0\times10^{-4}T - 3.0\times10^{-3}V + 0.65RH \quad (48)$$

$$R^2 = 0.996; \quad Adj\ R^2 = 0.995$$

The model equation was found to be highly significant (P<0.05) with a high R^2 value of 0.996 and an adjusted R^2 value of 0.995. Variance analysis revealed that the effects of drying air temperature, and relative humidity on the EIP were found to be highly significant (P<0.05).

The effect of drying air velocity, drying air temperature, and relative humidity on the exergetic sustainability index (ESI) of the native chili pepper drying chamber can be seen in Fig. 7(D) – (F). It could be observed that the ESI varied from 3.70-14.29; 5.18-14.29; and 14.29-5.43 for the corresponding drying air velocity range of 0.5-2 m/s (Fig. 7(D)); drying air temperature range of 40-70 ^oC (Figure 7(E)), and relative humidity of 60-75% (Fig. 9(F)). This shows that ESI increased with increasing drying air velocity and drying air temperature as well as decreased with increasing relative humidity. These observations illustrate that at higher exergetic efficiency values, there is an increase in the ESI which consequently results in a lower environmental impact. A similar report of an increase in ESI with increasing drying air temperature and drying air velocity has been presented by *Mondal et al.* [42] in the convective mixed flow drying of maize grain. A multivariate linear regression model equation fitted well to the ESI data and was found to be highly significant (P<0.05) with a high R^2 value of 0.960 and an adjusted R^2 value of 0.945. The empirical equation obtained from the fitting is expressed as follows:

$$ESI = 40.4 + 0.24T - 3.11V - 61.9RH \quad (49)$$

$$R^2 = 0.960; AdjR^2 = 0.945$$

The effects of drying air temperature, drying air velocity, and relative humidity on the ESI were found to be highly significant (P<0.05).

CONCLUSIONS

From this study, it can be deduced that to improve drying, energy, and exergetic efficiencies as well as save energy consumption in the course of convective cabinet hot air drying of red chili pepper there is the need to particularly control temperature and relative humidity. That is, higher drying, energy, and exergy efficiencies with a higher exergetic sustainability index as well as reduced energy consumption and heat loss during the drying of red chili pepper in a convective cabinet-tray dryer can be attained when drying conditions of higher air temperature, lower air velocity, and lower relative air humidity are utilized. For the convective cabinet hot air drying of red chili pepper, a drying air temperature of 70 ºC, air velocity of 0.5 m/s, and 60% relative humidity are the appropriate drying process conditions. Furthermore, the mass transfer models and the developed multivariate linear regression model examined in this study can be applied as significant tools for predicting and estimating drying parameters, moisture content profiles, and moisture transfer parameters. Similarly, the developed multivariate linear regression model can significantly and adequately be applied to predict the energy and exergetic parameters for convective cabinet hot air drying of chili pepper, since the prediction of these parameters and profiles is essential for practical drying applications, system design, analysis, and optimization. The exergetic improvement potential rates evaluation revealed that the drying chamber insulation is very critical for higher drying performance, especially at high temperatures. However, further studies will be performed to carry out exergo-economic and exergo-environmental analyses to facilitate the improvement of the cabinet-tray dryer performance as well as to perform an optimization study to find the optimal energy and exergy for the drying process.

Nomenclature

A_D	Surface area of drying equipment frame
AIC_C	Corrected Akaike Information Criterion
A_{Tr}	Tray area, m^2
b_o	Regression constant
b_1, b_2 and b_3	Coefficients of the parameters in multi-linear regression model
Bi	Biot number, dimensionless
C_{pda}	Specific heat of air, kJ/kg K
C_{mp}	Specific heat of moist product, kJ/kgK
C_{pwv}	Specific heat of water vapor, kJ/kgK
D_{eff}	Effective moisture diffusivity
Di	Dincer number, dimensionless
E_{AB}	Energy used by the air blower, kJ/s or kW
E_H	Energy transferred from heater to drying air, kJ/s
EIP	Exergetic improvement potential
ESI	Exergetic sustainability index
EUR	Energy utilization ratio, dimensionless
ex	Specific exergy, kJ/kg
ex_{aci}	Specific exergy inflow into the drying chamber, kJ/kg
ex_{dco}	Specific exergy outflow from the drying chamber, kJ/kg
ex_{wc}	Specific exergy of water content, kJ/kg
ex_{mp}	Specific exergy of moist product, kJ/kg
$\dot{E}x$	Exergy rate, kJ/s or kW
$\dot{E}x_{des}$	Exergy rate of destruction or irreversibility, kJ/s or kW
$\dot{E}x_{evap}$	Exergy rate for moisture evaporation, kJ/s or kW
$\dot{E}x_{in}$	Exergy inflow rate, kJ/s or kW
$\dot{E}x_{out}$	Exergy outflow rate, kJ/s or kW
$\dot{E}x_{Loss}$	Exergy loss rate, kJ/s or kW
Fo	Fourier number, dimensionless
G	Lag factor
H	Enthalpy, kJ/kgK
HDT	Half-drying time
h_{dai}	Enthalpy of inlet drying air, kJ/kg
h_{dao}	Enthalpy of outlet drying air, kJ/kg
h_{FP}	Enthalpy of fresh chili pepper, kJ/kg
h_{DP}	Enthalpy of dried chili pepper product, kJ/kg
h_f	Enthalpy of saturated water, kJ/kgK
h_g	Enthalpy of saturated vapor, kJ/kgK
h_v	Latent heat of vaporization, kJ/kg
K_m	Mass transfer coefficient, m/s
L	Length of chili pepper sample, m

M	Moisture content of the wet sample, wet basis
M_o	Initial moisture content (kg water/kg dry matter) at time t= 0
M_t	Moisture content (kg water/kg dry matter) at time t=t
M_{eq}	Equilibrium moisture content, kg water/kg dry matter
MR	Normalized moisture content or dimensionless moisture ratio
m_w	Mass of evaporated water from samples, kg
$\dot{m}$	Mass flow rate, kg/s
$\dot{m}_{dai}$	Mass flow rate of inlet drying air, kg/s
$\dot{m}_{dao}$	Mass flow rate of outlet drying air, kg/s
$\dot{m}_{FP}$	Mass flow rate of fresh chili pepper
$\dot{m}_{DP}$	Mass flow rate of dried chili pepper product, kg/s
$\dot{m}_{wc}$	Mass flow rate of water content, kg/s
η_D	Drying efficiency, %
η_E	Energy efficiency, %
η_{Ex}	Exergy efficiency, %
P	Atmospheric pressure, kPa
P_{vs}	Saturated vapor pressure, kPa
ρ_{da}	Density of drying air medium, kg/m^3
Q_m	Energy utilized for heating the sample, kJ
Q_w	Energy consumed for moisture evaporation, kJ
$\dot{Q}_{Loss}$	Rate of heat loss by the drying equipment, kJ/s
ϕ	Relative humidity, %
RMSE	Root mean square error
R^2	Coefficient of determination
R_{da}	Gas law constant for drying air, kJ/kgK
R_{wv}	Gas law constant for water vapour, kJ/kgK
RH	Relative humidity, %
S	Drying coefficient, s^{-1}
s_f	Entropy for saturated water, kJ/kg/K
s_g	Entropy for saturated vapor, kJ/kg/K
SEC	Specific energy consumption, MJ/kg
T	Absolute temperature, K
T_{dav}	Average value of the temperature measured at three different points of dryer's body
T_i and T_o	Inlet and outlet temperature of food material (K), respectively
T_p	Temperature of moist chili pepper product, ^oC
T_∞	Ambient air temperature, ^oC
ΔT	Temperature difference between the inlet drying temperature and sample temperature
t_T	Total drying time, s
TEC	Total energy consumption, MJ
U_D	Heat loss transfer coefficient or thermal loss factor of drying equipment, kW/m^2 ^oC
μ_l	Characteristic root or coefficient, dimensionless
V	Air velocity, m/s
V_{da}	Velocity of drying air, m/s
ν	Dynamic viscosity of drying air medium, kg/ms
W_m	Weight of the dried product, kg
w	Humidity ratio, kg water/kg dry air
X_i	Actual value of the variable
X_{mean}	Mean or average of the measurements
X_1, X_2 and X_3	Independent variables representing drying air temperature, drying air velocity, and relative humidity, respectively.
x^o_{wv}	Mole fraction of water vapor in the air
∂X_i	Uncertainty in the measurement
Y	Response variable
y	Half-thickness of sample, m
λ_A	Relative Akaike Weight, RAW

Received :May 27, 2021 ; Accepted : Aug. 30, 2021

REFERENCES

[1] Olatunji T. L., Afolayan A. J., The Suitability of Chili Pepper (*Capsicum Annuum* L.) for Alleviating Human Micronutrient Dietary Deficiencies: A review, *Food Sci. Nutri.*, **6(8)**: 2239-2251 (2018).

[2] Giuff rida D., Dugo P., Torre G., Bignardi C., Cavazza A., Corradini C., Dugo G., Characterization of 12 Capsicum Varieties by Evaluation of their Carotenoid Profile and Pungency Determination, *Food Chem.*, **140**: 794-802 (2013).

[3] Arun S., Yashwanth N., Adharsh R., Experimental and Comparison Studies on Drying Characteristics of Red Chillies in a Solar Tunnel Greenhouse Dryer and in the Open Sun Drying Method, *Int. J. Inventive Eng. Sci.*, **2(11)**: 2319–9598 (2014).

[4] Mihindukulasuriya S. D. F., Jayasuriya H. P. W., Drying of Chilli in A Combined Infrared and Hot Air Rotary Dryer, *J. Food Sci. Technol.*, **52(8)**: 4895–4904 (2015).

[5] Tunde-akintunde T.Y., Afolabi, T.J., Drying of Chili Pepper *(Capscium frutscens)*. *J. Food Proc. Eng.*, **33(4)**: 649-660 (2010).

[6] Saengrayap R., Boonlap N., Boonsorn U., Effect of Pre-Treatment Methods on the Color Changes during Drying of Red Chilli (*Capsicum frutescens* L.), *Proc. of MATEC Web of Conferences* **62:** 02009 (2016).

[7] Montoya-Ballesteros L.C., Gonz´alez-Le´on A., Mart´ınez-N´u˜nez Y.J., Robles-Burgue˜no M.R., Garc´ıa-Alvarado M.A., Rodr´ıguez-Jimenes G. C., Impact of Open Sun Drying and Hot Air Drying on Capsaicin, Capsanthin, and Ascorbic Acid Content in Chiltepin (*Capsicum Annuum L. Var. Glabriusculum*), *Revista Mexicana de Ingeniería Química*, **16(3)**: 813-825 (2017).

[8] Artnaseaw A., Theerakulpisut S., Chatchai B., Development of a Vacuum Heat Pump Dryer for Drying Chilli, *Biosystem Eng.*, **105**: 130-138 (2010).

[9] Tavakolipour H., Mokhtarian M., Drying of Chilli Pepper in Various Conditions, *Quality Assur. Saf. Crops & Foods*, **8(1)**: 87-93 (2015).

[10] Mihindukulasuriya S.D.F., Jayasuriya H.P.W., Mathematical Modeling of Drying Characteristics of Chilli in Hot Air Oven and Fluidized Bed Dryers, *Agric Eng Int CIGR J.*, **15**: 154–166 (2013).

[11] Agrawal S.G., Methekar R. V., Mathematical Model for Heat and Mass Transfer during Convective Drying of Pumpkin, *Food Bioprod Process.*, **101**: 68-73 (2016).

[12] Salehi F., Kashaninejad M., Modeling of Moisture Loss Kinetics and Color Changes in the Surface of Lemon Slice during the Combined Infrared-Vacuum Drying, *Informat. Process Agric.*, **5(4)**: 516 – 523 (2018).

[14] Khanali M., Banisharif A., Rafiee S., Modeling of Moisture Diffusivity, Activation Energy and Energy Consumption in Fluidized Bed Drying of Rough Rice, *Heat Mass Transf.*, **52**: 2541-2549 (2016).

[13] Md Saleh R., Kulig B., Hensel O., Sturm B., 1nvestigation of Dynamic Quality Changes and Optimization of Drying Parameters of Carrots (*Daucus carota var. laguna*), *J. Food Proc. Eng.*, e13314 (2019).

[15] Darvishi H., Quality, Performance Analysis, Mass Transfer Parameters and Modeling of Drying Kinetics of Soybean, *Braz. J. Chem. Eng.*, **34(1)**: 143-158 (2017).

[16] Mohammadi I., Tabatabaekoloor R., Motevali A., Effect of Air Recirculation and Heat Pump on Mass Transfer and Energy Parameters in Drying of Kiwifruit Slices, *Energy*, **170**: 149–158 (2019).

[17] Akpinar E.K., Dincer, I., Application of Moisture Transfer Models to Solids Drying, *Proc. IMechE J. Power Energy*, **219** Part A: 235-244 (2005).

[18] Liu X, Hou H, Chen J., Applicability of Moisture Transfer Parameters Estimated by Correlation between Biot Number and Lag Factor (Bi–G Correlation) for Convective Drying of Eggplant Slices, *Heat Mass Transf.*, **49**: 1595-1601 (2013).

[19] Darvishi H., Asl A.R., Asghari A., Azadbakht M., Najafi G., Khodaei J., Study of the Drying Kinetics of Pepper, *J. Saudi Soc. Agric. Sci.*, **13**: 130-138 (2014).

[20] Beigi M., Energy Efficiency and Moisture Diffusivity of Apple Slices During Convective Drying, *Food Sci. Technol.*, **36(1)**: 145-150 (2016).

[21] Darvishi H., Zarein M., Farhudi Z., Energetic and Exergetic Performance Analysis and Modeling of Drying Kinetics of Kiwi Slices, *J. Food Sci. Technol.*, **53(5)**: 2317–2333 (2016).

[22] Tunde-Akintunde T.Y., Effect of Pretreatments on Drying Characteristics and Energy Requirements of Plantain (*Musa Aab*). *J. Food Proc. Preserv.*, **38**: 1849-1859 (2014).

[23] Torki Harchegan M., Sadeghi M., Ghanbarian D., Moheb A., Dehydration Characteristics of Whole Lemons in a Convective Hot Air Dryer, *Iran. J. Chem. Chem. Eng. (IJCCE)*, **35 (3)**: 65-73 (2016).

[24] Ju H.-Y., El-Mashad H. M., Fang X.-M., Pan Z., Xiao H.-W., Liu Y.-H., Gao Z.-J., Drying Characteristics and Modeling of Yam Slices under Different Relative Humidity Conditions, *Drying Technol.*, **34(3)**: 296–306 (2016).

[25] Abbaszadeh A., Motevali A., Ghobadian B., Khoshtaghaza M.H., Minaei S., Effect of Air Velocity and Temperataure on Energy and Effective Moisture Diffusivity for Russian Olive (*Elaeagnusan Gastifolial* L.) in Thin-Layer Drying, *Iran. J. Chem. Chem. Eng. (IJCCE)*, **31(1)**: 75-79 (2012).

[26] Zakipour E., Hamidi Z., Vacuum Drying Characteristics of Some Vegetables, *Iran. J. Chem. Chem. Eng. (IJCCE)*, **30(4)**: 97-105 (2011).

[27] Erbay Z., Icier F., Energy and Exergy Analyses on Drying of Olive Leaves *(olea europaea* l.) in Tray Drier, *J. Food Proc. Eng.*, **34**: 2105–2123 (2011).

[28] Castro M., Román C., Echegaray M., Mazza G., Rodriguez R., Exergy Analyses of Onion Drying by Convection: Influence of Dryer Parameters on Its Performance, *Entropy*, **20**: 310-314 (2018).

[29] Lingayat A., Chandramohan V.P., Raju V.R.K., Energy and Exergy analysis on Drying of Banana using Indirect Type Natural Convection Solar Dryer, *Heat Transfer Eng.*, **41(6-7)**: 551-561 (2020).

[30] Prommas R., Rattanadecho P., Jindarat W., Energy and Exergy Analyses in Drying Process of Non-Hygroscopic Porous Packed Bed Using a Combined Multi-Feed Microwave-Convective Air and Continuous Belt System (CMCB), *Heat Mass Transf.*, **39**: 242–250 (2012).

[31] Akpinar E.K., Energy and Exergy Analyses of Drying of Red Pepper Slices in Convective Type Dryer, *Int. Comm. Heat Mass Transf.*, **31(8)**: 1165–1176 (2004).

[32] Corzo O., Bracho N., Vasquez A., Pereira, A., Energy and Exergy Analyses of Thin Layer Drying of Coroba Slices, *Food Eng.*, **86(2)**: 151–161 (2008).

[33] Folayan J. A., Osuolale F. N., Anawe A. L., Data on Exergy and Exergy Analyses of Drying Process of Onion in a Batch Dryer, *Data in Brief*, **21**: 1784-1793 (2018).

[34] Nazghelichi T., Kianmehr M., Aghbashlo M., Thermodynamic Analysis of Fluidized Bed Drying of Carrot Cubes, *Energy*, **35(12)**: 4679-4684 (2010).

[35] Rabha D., Muthukumar, D., Somayaji C., Energy and Exergy Analyses of the Solar Drying Processes of Ghost Chilli Pepper and Ginger, *Renew. Energy*, **105**: 764-773 (2017).

[36] Agarry S.E., Modelling the Drying Characteristics and Kinetics of Hot Air-Drying of Un-Blanched Whole Red Pepper and Blanched Bitter Leaf Slices, *Turkish J. Agric- Food Sci. Technol.*, **5(1)**: 24-32 (2017).

[37] Deng L.-Z., Yang X.-H., Mujumdar A. S., Zhao J.-H., Wang D., Zhang Q., Xiao H.-W., Red Pepper (*Capsicum Annuum* L.) Drying: Effects of Different Drying Methods on Drying Kinetics, Physicochemical Properties, Antioxidant Capacity, and Microstructure, *Drying Technol.*, **36(8)**: 893-907 (2018).

[38] Kumara V., Shrivastava, S.L., Vacuum-Assisted Microwave Drying Characteristics of Green Bell Pepper, *Int. J. Food Studies*, **6**: 67-81 (2017).

[39] Arslan D., Ozcan M.M., Dehydration of Red Bell-Pepper (*Capsicum Annuum* L.): Change in Drying Behavior, Colour and Antioxidant Content, *Food Bioprod. Process*, **89**: 504-513 (2011).

[40] Pavani S., Vani V.S., Dorajee Rao A.V.D., Viji C.P., Suneetha D.R.S., Subbaiah K.V., Kiran Kumar G.N., Sarada P., Influence of Pre-Treatments and Drying Methods on Physico-Chemical Characteristics of Green Chilli Powder, *Int. J. Pure App. Biosci.*, **6(2)**: 1148-1152 (2018).

[41] Kamal M.M., Ali M.R., Rahman M.M., Shishir M.R.I, Yasmin S., Sarker Md.S.H., Effects of Processing Techniques on Drying Characteristics, Physicochemical Properties and Functional Compounds of Green and Red Chilli (*Capsicum annum L.*) Powder, *J. Food Sci. Technol.*, **56**: 3185–3194 (2019).

[42] Mondal Md. H.T., Hossain Md. A., Sheik Md. A.M., Akhtaruzzaman Md., Sarker Md.S.H., Energetic and Exergetic Investigation of a Mixed Flow Dryer: A Case Study of Maize Grain Drying, *Drying Technol.*, 1-16 (2020).

[43] Kaveh M., Karami H., Jahanbakhshi A., Investigation of Mass Transfer, Thermodynamics, and Greenhouse Gases Properties in Pennyroyal Drying, *J. Food Proc. Eng.*, e13446 (2020).

[44] Agnihotri V., Jantwal A., Joshi, R., Determination of Effective Moisture Diffusivity, Energy Consumption and Active Ingredient Concentration Variation in *Inula racemosa*, Rhizomes During Drying, *Ind. Crop Prod.*, **106**: 40-47 (2017).

[45] Dincer I., Sahin A.Z., A New Model for Thermodynamic Analysis of a Drying Process, *Int. J. Heat Mass Transf.*, **47(4)**: 645-652 (2004).

[46] Román F., Hensel O., Effect of Air Temperature and Relative Humidity on The Thin-Layer Drying of Celery Leaves *(Apium Graveolens Var. Secalinum)*, *Agric. Eng. Int.: the CIGR J.*, **13(2)**: 1-11 (2011).

[47] Pankaew P., Janjai S., Nilnont W., Phusampao C., Bala B.K., Moisture Desorption Isotherm, Diffusivity and Finite Element Simulation of Drying of Macadamia Nut (*Macadamia integrifolia*), *Food Bioprod. Process.*, **100**: 16–24 (2016).

[48] Taheri-Garavand A., Meda V., Drying Kinetics and Modeling of Savory Leaves Under Different Drying Conditions, *Int. Food Res. J.*, **25(4)**: 1357-1364 (2018).

[49] Agarry S.E., Osuolale F.N., Agbede O.O., Ajani A.O., Afolabi T.J., Ogunleye O.O., Ajuebor F., Owabor C.N., Transport Phenomena, Thermodynamic Analyses, and Mathematical Modelling of Okra Convective Cabinet-Tray Drying at Different Drying Conditions, *Eng. & Appl. Sci. Res*., **48(5)**: 637-656 (2021).

[50] Herman C., Spreutels L., Turomzsa N., Konagano E. M., Haut B., Convective Drying of Fermented Amazonian Cocoa Beans (Theobroma Cacao Var. Forasteiro). Experiments and Mathematical Modeling, *Food Bioprod. Process.*, **108**: 81-94 (2018).

[51] AOAC, (Association of Official Analytical Chemists). "Official Methods of Analysis". 16th ed. Washington DC, pp. 202 (2015).

[52] Dincer I., Dost S. A., Modelling Study for Moisture Diffusivities and Moisture Transfer Coefficients in Drying of Solid Objects, *Int. J. Energy Res.*, **20**: 531-539 (1996).

[53] Akpinar E. K, Toraman S., Determination of Drying Kinetics and Convective Heat Transfer Coefficients of Ginger Slices, *Heat Mass Transf.*, **52**: 2271-2281 (2016).

[54] Aghbashlo, M., Kianmehr, M., Arabhosseini, A. (2008). Energy and Exergy Analyses of Thin-Layer Drying of Potato Slices in a Semi-Industrial Continuous Band Dryer, *Drying Technol*., **26**: 1501–1508 (2008).

[55] Zeki B., Physical Properties of Food Materials. In: "Food Process Engineering and Technology", 1-26. Elsevier Publishers, USA (2009).

[56] Minaei S., Chenarbon H. A., Motevali A., Hosseini A.A., Energy Consumption, Thermal Utilization Efficiency and Hypericin Content in Drying Leaves of St John's Wort (*Hypericum Perforatum*), *J. Energy in Southern Africa*, **25(3)**: 27-35 (2014).

[57] Chen C., Venkitasamy C., Zhang W., Deng L., Meng X., Pan Z., Effect of Step-Down Temperature Drying on Energy Consumption and Product Quality of Walnuts, *J. Food Eng.*,**285**: 110105 (2020)

[58] Afolabi T. J., Agarry S. E., Thin Layer Drying Kinetics and Modelling of Okra (*Abelmoschus Esculentus* (L.) *Moench*) Slices under Natural and Forced Convective Air Drying, *Food Sci. Quality Manage.*, **28**: 35-50 (2014).

[59] Ozgen F., Celik N., Evaluation of Design Parameters on Drying of Kiwi Fruit, *Appl. Sci.*, **9(10)**: 1-13 (2019).

[60] Barati E., Esfahani J.A., A Novel Approach to Evaluate the Temperature during Drying of Food Products with Negligible External Resistance to Mass Transfer, *J. Food Eng.*, **114**: 39-46 (2013).

[61] Mujaffar S., John S., Thin-Layer Drying Behavior of West Indian Lemongrass (*Cymbopogan Citratus*) Leaves, *Food Sci. Nutri*., **6**: 1085-1099 (2018).

[62] Ju H-Y., Zhao S-H., Mujumdar A. S., Zhao H-Y., Duan X., Zheng Z-A., Gao Z-J., Xiao H-W., Step-Down Relative Humidity Convective Air Drying Strategy to Enhance Drying Kinetics, Efficiency, and Quality of American Ginseng Root (*Panax quinquefolium*), *Drying Technol.*, **38(7)**: 903-916 (2020).

[63] Nwakuba N.R., Chukwuezie O. C., Osuchukwu L. C., Modeling of Drying Process and Energy Consumption of Onion (Ex-gidankwano Spp.) Slices in a Hybrid Crop Dryer, *Amer. J. Eng. Res.*, **6(1)**: 44-55 (2017).

[64] Azadbakht M., Torshizi M., Ziaratban A., Aghili H., Energy and Exergy Analyses during Eggplant Drying in a Fluidized Bed Dryer, *Agric. Eng. Int.: CIGR J.*, **19(3)**: 177-182 (2017).

[65] Motevali A., Minaei S., Banakar A., Ghobadian B., Khoshtaghaza M.H., Comparison of Energy Parameters in Various Dryers, *Energy Convers. Manage.*, **87**: 711-725 (2014).

[66] Motevali A., Minaei S., Banakar A., Ghobadian B., Darvishi H., Energy Analyses and Drying Kinetics of Chamomile Leaves in Microwave-Convective Dryer, *J. Saudi Soc. Agric. Sci.*, **15**: 179-187 (2016).

[67] Icier F., Colak N., Erbay Z., Kuzgunkaya E. H., Hepbasli A.A., Comparative Study on Exergetic Performance Assessment for Drying of Broccoli Florets in Three Different Drying Systems, *Drying Technol.*, **28**: 193-204 (2010).